Russian Geology and Geophysics © 2019, V.S. Sobolev IGM, Siberian Branch of the RAS
Vol. 60, No. 10, pp. 1101–1118, 2019 *DOI:10.15372/RGG2019112* *Geologiya i Geofizika*

Paleoproterozoic Metavolcanosedimentary Sequences of the Yenisei Metamorphic Complex, Southwestern Siberian Craton (Angara–Kan Block): Subdivision, Composition, and U–Pb Zircon Age[1]

A.D. Nozhkin[a,b,] ✉, O.M. Turkina[a,b], I.I. Likhanov[a], K.A. Savko[c]

[a] *V.S. Sobolev Institute of Geology and Mineralogy, Siberian Branch of the Russian Academy of Sciences, pr. Akademika Koptyuga 3, Novosibirsk, 630090, Russia*

[b] *Novosibirsk State University, ul. Pirogova 2, Novosibirsk, 630090, Russia*

[c] *Voronezh State University, Universitetskaya pl. 1, Voronezh, 394006, Russia*

Received 15 August 2018; received in revised form 16 January 2019; accepted 21 March 2019

Abstract—The results of this study reveal the chemical heterogeneity of the Yenisei metamorphic complex, which is a series of blocks within the Yenisei Fault of the southern Yenisei Ridge (Angara–Kan block). The Yenisei complex is composed of four metamorphic sequences: amphibolite–marble–paragneiss (volcanic–carbonate–terrigenous), amphibolite–orthogneiss (volcanic), marble–paragneiss (carbonate–terrigenous), and paragneiss (terrigenous). Study of the nature of the protoliths of metamorphic rocks shows that gneisses and schists of Sequences I and IV correspond to polymict or arkose sandstones and siltstone–mudstones and can be classified as first-cycle sediments. Garnet–two-mica schists of Sequence III correspond in composition to mudstones and show evidence of recycling. Metavolcanic sequence II is composed of andesite–dacite–trachyrhyodacite, leucobasalt–basalt, and basalt–basaltic-andesite–trachyandesite formations. The metasedimentary rocks are 1.2–1.4 times richer in REE and Th than the average PAAS. The high-alumina varieties have high contents of K, Rb, HFSE, Fe, Cr, Ni, and Co. The total similarity of the average trace-element contents in the rocks of the two complexes suggests that the composition of the Kan granulites was inherited by metasedimentary rocks of the Yenisei complex. The U–Pb zircon dates for granite veins cutting gneisses of amphibolite–marble–paragneiss Sequence I limit the deposition age to 1.84–1.85 Ga and indicate that these rocks were deposited before the emplacement of postcollisional granites of the Taraka massif and thus predate the major orogenic events within the Angara–Kan block. Therefore, these rocks can be correlated with the lower part of the Urik–Iya graben section. The metamorphic rocks from the lower parts of the sections of the Yenisei complex and the Subluk Group formed during the same rifting phase of sedimentation. The amphibolite–orthogneiss (volcanic) sequence formed in the Angara–Kan block of the Yenisei Ridge during the second stage (1.74 Ga). The volcanic rocks formed in an extension setting and thus can be correlated with the emplacement of within-plate granites of the Taraka massif. In the Sayan area, terrigenous sediments and volcanic rocks of various compositions accumulated at the second stage (1.75–1.70 Ga) during the intracontinental extension. Therefore, there is a good correlation between the ages and geodynamic settings of deposition of late Paleoproterozoic volcanic and volcanosedimentary complexes of the Yenisei Ridge and the Sayan region.

Keywords: paragneisses, subdivision, geochemistry, U–Pb age, Paleoproterozoic, geodynamics, correlation, Angara–Kan block

INTRODUCTION

The Angara fold belt, extending over 1400 km and embracing metamorphic sedimentary and volcanic rocks of the Yenisei Ridge and Sayan region (Fig. 1) (Nozhkin, 1999; Dmitrieva and Nozhkin, 2012) has originated in the late Paleoproterozoic at the western margin of the Siberian craton. In the south of the Yenisei Ridge, within the Angara–Kan block, the Paleoproterozoic stage was marked by the formation of the Yenisei schist-gneiss complex (Fig. 2). To the north, in the Transangarian part, gneisses and crystalline schists are exposed in the Yenisei and Central horsts (Postel'nikov, 1980) and are referred to as the pre-Riphean Garevka complex. The metamorphic strata of the Garevka complex (Kachevskii et al., 1994; Kachevskii, 2002) are composed of biotite and biotite-amphibole plagiogneisses, aluminous garnet-sillimanite and two-mica schists, horizons of quartzites and metaterrigenous-carbonate rocks. To the east, the Panimba uplift abounds in metamorphosed aluminous terrigenous and clay-carbonate rocks of the Teya Group unconformably overlain by the Lower–Middle Riphean metaterrigenous strata of the Sukhoi Pit Group. In the southeastern extension of the Angara belt, Paleoproterozoic rocks are extensively distributed within the Sayan uplift. The Tumanshet trough, a large sedimentary basin on the western margin of the Biryusa block (Galimova and Bormotkina, 1983; Sez'ko, 1988; Gerya et al., 1997; Dmitrieva

[1] This paper was translated by the authors.

✉ Corresponding author.
E-mail adress: nozhkin@igm.nsc.ru (A.D. Nozhkin)

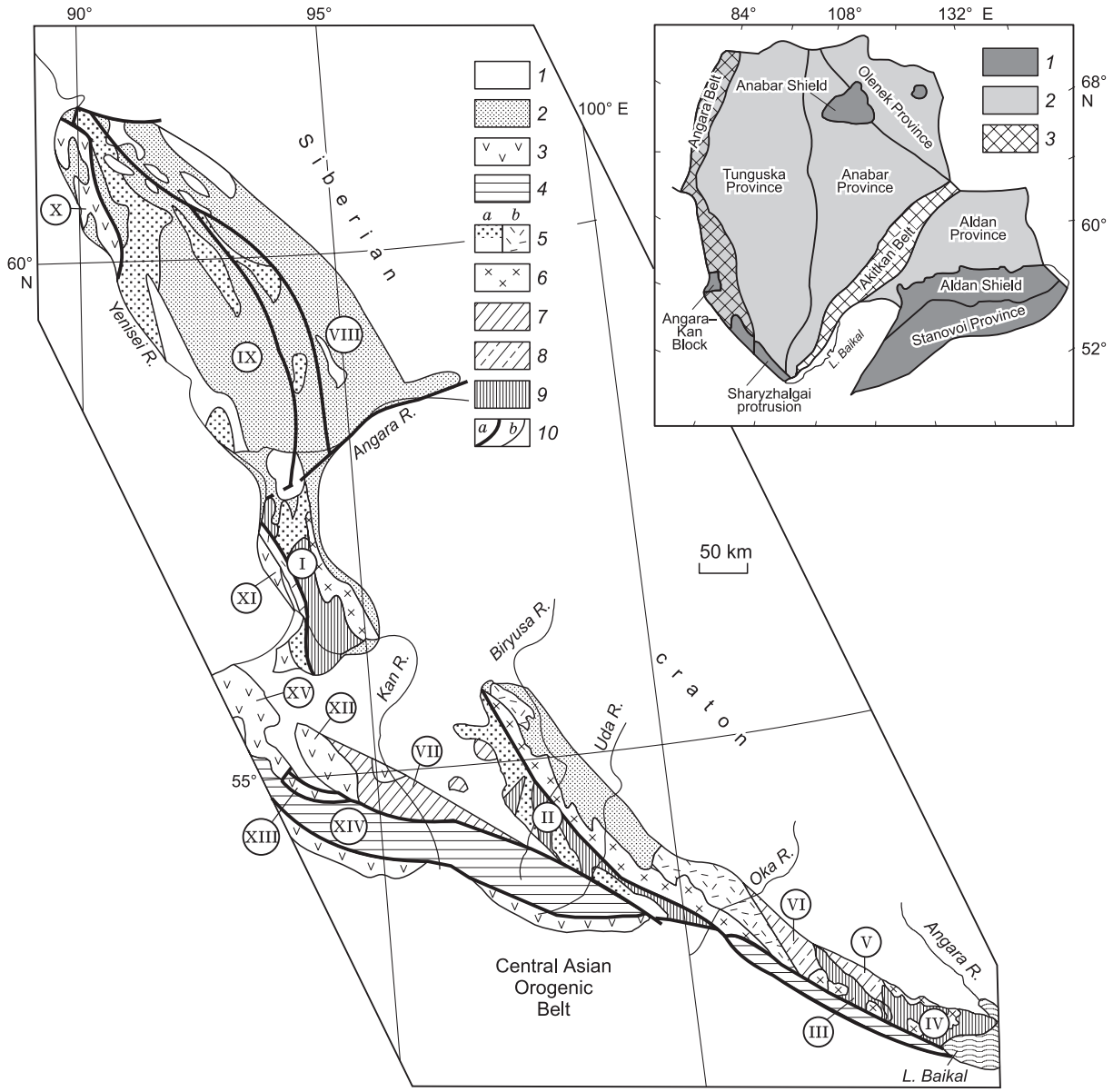

Fig. 1. Schematic map showing the distribution of Paleoproterozoic complexes at the southwestern margin of the Siberian craton. Compiled by A.D. Nozhkin. *1*, platform cover deposits; *2*, Riphean continental marginal complexes; *3*, Riphean paleo-oceanic and paleo-island-arc accretionary complexes; *4*, Vendian metaterrigenous-carbonate complexes of the Derba microcontinent and the Kitoikina zone; *5*, Paleoproterozoic continental marginal complexes of the Angara fold belt (AFB): metasedimentary (*a*), metavolcanosedimentary (*b*); *6*, Paleoproterozoic granitoid complexes of the Angara collisional orogen; *7*, Paleoproterozoic complexes of greenstone belts; *8*, Archean tonalite-trondhjemite-granodiorite and greenstone belt complexes; *9*, Archean granulite-gneiss complexes; 10, faults (*a*), other geologic boundaries (*b*). Blocks: I, Angara–Kan; II, Biryusa; III, Kitoi; IV, Irkut; V, Onot; VI, Ermin; VII, Kan; VIII, Eastern; IX, Central; X, Isakovka; XI, Predivinsk; XII, Shumikha–Kirel; XIII, Arzybei; XIV, Derba; XV, Kuvai. Inset shows the main tectonic elements of the Siberian Craton, after Rosen et al. (1994) and Donskaya et al. (2009). *1*, basement highs; *2*, buried basement; *3*, Paleoproterozoic orogenic belts.

and Nozhkin, 2012) is filled with substantially metaterrigenous deposits of the Neroi Group, which, in turn, rest with stratigraphic unconformity upon Archean highly metamorphosed rocks of the Khailama complex (Galimova and Bormotkina, 1983). The Urik–Iya and Elash grabens filled with metavolcanic-terrigenous complexes of the Subluk and Elash groups (Geological Map..., 1985; Bryntsev, 1994; Perfil'eva and Galimova, 1998; Galimova et al., 2011) occur along the northeastern margin of the Sayan uplift and are unconformably overlain by late Neoproterozoic deposits of the Karagass and Oselok Groups.

Evidence for the structural setting of the Angara fold belt along the continental margin is clearly provided by linear belts of granitic intrusions of the Yenisei Ridge and Sayan area (Fig. 1). Folding and metamorphism of stratified rock units and subsynchronous granitoid magmatism occurred at

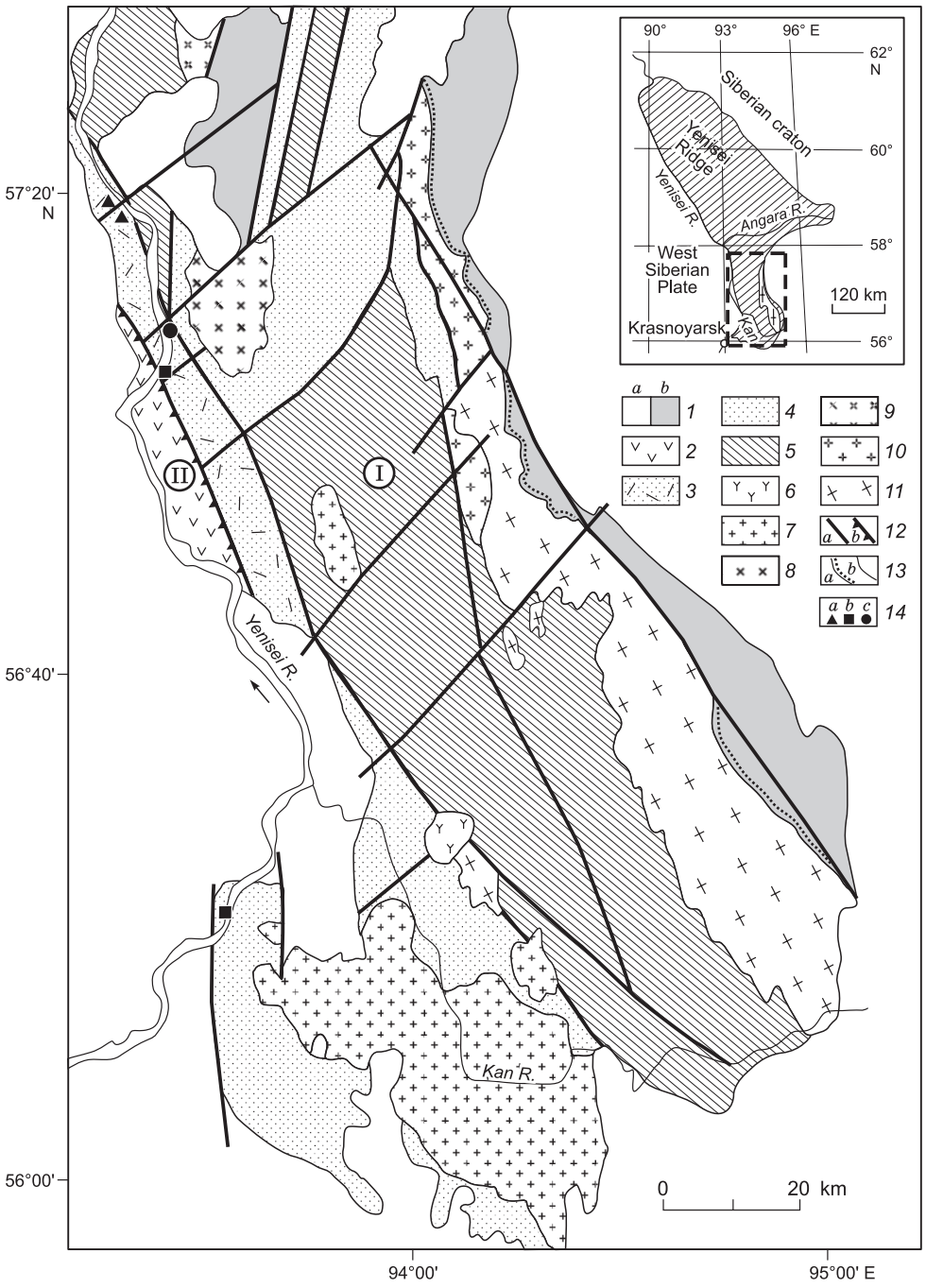

Fig. 2. Schematic geological map of the Angara–Kan block (Yenisei Ridge), modified after Nozhkin and Turkina (1993), Popov (2001), and Vernikovskaya et al. (2010). *1*, overlying Phanerozoic (*a*) and Neoproterozoic (*b*) sediments; *2*, ophiolite and island-arc complexes of the Predivinsk terrane (NP_3); *3–5*, metamorphic complexes of the Angara–Kan block: *3*, metavolcanosedimentary, *4*, essentially metasedimentary rocks of the Yenisei schist-gneiss (PP_4), *5*, Kan granulite-gneiss (AR?) complexes; *6*, alkaline syenites and trachytes ($T_{1–2}$), rhyolites and leucogranites (D_2) of the Severnyi volcanotectonic depression; *7*, granitoids of the Nizhnii Kan pluton (O_3); *8*, porphyroblastic gneissic granites, granites, syenites of the Posol'nyi pluton (PP_4?, $Є_{1–2}$); *9*, subalkaline granites, leucogranites of the Chistoe Pole pluton (NP_2); *10*, subalkaline granites, leucogranites (PP_4); *11*, gneissic granites, plagiogranites, porphyritic granites (PP_3) of the Taraka pluton; *12*, faults (*a*), thrusts (*b*); *13*, unconformity (*a*), other boundaries (*b*); *14*, sampling sites for U–Pb dating of volcanics (*a*), granites (*b*) and sedimentary rocks (c). I, Angara–Kan block; II, Predivinsk terrane. Inset shows the contours of the map in Fig. 1.

~1.84–1.87 Ga (Levitskii et al., 2002; Nozhkin et al., 2003; Turkina et al., 2006; Urmantseva et al., 2012; Donskaya et al., 2014; Turkina and Sukhorukov, 2015). Stratified rocks were metamorphosed to greenschist through epidote-amphibolite and amphibolite facies (Gladkochub et al., 2014; Likhanov et al., 2015b; Nozhkin et al., 2016).

Although Paleoproterozoic deposits have a wide lateral distribution, the evidence on their formation conditions and age position is more or less fragmentary, and correlation of the variably metamorphosed strata remains controversial. This paper reports new data on subdivision, Sm–Nd isotopic systematics, U–Pb zircon age of metasedimentary rocks and granitoids of the Yenisei metamorphic complex of the Angara–Kan block (Yenisei Ridge), which can be correlated with Paleoproterozoic deposits from the other parts of the Angara fold belt.

GEOLOGICAL SETTING OF THE YENISEI METAMORPHIC COMPLEX IN THE STRUCTURE OF THE ANGARA–KAN BLOCK OF THE YENISEI RIDGE AND THE PROBLEM OF ITS SUBDIVISION

The Yenisei Ridge is divided into two large segments, the South Yenisei and Transangarian, separated by the N–S-trending Lower Angara Fault (Fig. 1). Two structural elements have been recognized south of this fault, the early Precambrian Angara–Kan block, formed by the Kan granulite-gneiss and Yenisei schist-gneiss complexes and granitoids, and the Neoproterozoic Predivinsk island-arc terrane. North of the Lower Angara fault in the Transangarian part, the Yenisei Ridge is composed of Paleoproterozoic and Meso-Neoproterozoic rocks of the East (periplatform) and Central cratonic blocks and Isakovka (western) terrane, composed of Neoproterozoic ophiolites and island-arc complexes (Likhanov and Santosh, 2017). All tectonic blocks and terranes are separated by regional faults having general NW-strike and subvertical dip. The largest one is the Yenisei Fault Zone, which is interpreted as a continuation of the Baikal–Yenisei Fault (the Major fault zone of Eastern Sayan) and, therefore, is a structure bounding the Siberian Craton in the west (Likhanov and Santosh, 2019).

The Kan granulite-gneiss and Yenisei schist-gneiss complexes of Archean age were identified in the Angara–Kan block (Kuznetsov, 1988). Their Archean age is indicated in the legend to the present map (Kachevskii, 2002) as well as in previous geological maps. The age of the protoliths of the Kan complex remains controversial due to repeated pulses of high-temperature metamorphism. The Nd model age data for most paragneisses indicate that they were formed in the late Archean (Nozhkin et al., 2008). The age of the early Paleoproterozoic granulite-facies metamorphism of the Kan complex was estimated between 1.9 Ga (Bibikova et al., 1993) and 1.87–1.85 Ga (Urmantseva et al., 2012; Turkina and Sukhorukov, 2015). Granulite-facies metamorphism and subsequent granite emplacement were associated with the formation of the Angara collisional orogen (Nozhkin, 1999) and correspond to the timing of the final accretion of the Siberian Craton.

The Kan granulite-gneiss complex constitutes the main part of the area of the Angara–Kan block and comprises two sequences (Kuzeeva and Atamanovo). The Kuzeeva sequence is dominated by garnet-biotite-hypersthene gneisses and, more rarely, aluminous gneisses with cordierite, sillimanite and spinel, garnet-two-pyroxene schists and charnockites. The Atamanovo sequence is dominated by migmatized garnet-biotite and aluminous gneisses. The average composition of the Kan complex corresponds to granodiorite (Nozhkin and Turkina, 1993) and is close to the composition of the post-Archean upper continental crust (Taylor and McLennan, 1988). The Nd model age for aluminous gneisses (2.5 to 2.8 Ga) (Nozhkin et al., 2008) confirms presupposes the late Archaean age of their terrigenous source. For the garnet-cordierite-sillimanite-quartz assemblage in paragneisses, the peak metamorphic *P–T* conditions are estimated to be 780–795 °C and 6.1 kbar for the western and 716 °C and 4.5 kbar for the eastern parts of the Angara–Kan block (Perchuk et al., 1989). Temperature estimates from two-pyroxene mafic granulites vary between ~800–870 and 900 °C, and *P–T* parameters for garnet coronites in them are estimated at 750–860 °C and 8.0–9.5 kbar (Turkina and Sukhorukov, 2015). The evidence for ultrahigh-temperature (UHT) granulite metamorphism has been recently reported from metapelites of Fe–Al composition with peak temperatures of 900–1000 °C on the right bank of the Yenisei River, which are mainly composed of garnet–hypersthene–sillimanite–cordierite–plagioclase–biotite–spinel–quartz–K-feldspar assemblage (Likhanov et al., 2015c) sometimes containing sapphirine (Sukhorukov et al., 2018a, b). The observed counterclockwise *P–T* metamorphic evolution of rocks along a high geothermal gradient (dT/dP = 100–200 °C/kbar) suggests that UHT metamorphic assemblages were formed in an overall extensional tectonic setting, accompanied by underplating of mantle-derived mafic magmas. This confirms the previous ideas about the two-stage evolution of granulite-facies metamorphism in the Angara–Kan block that was controlled by different tectonic processes. The first stage (1.89–1.87 Ga) was almost contemporaneous with collisional processes and emplacement of post-collisional granites at 1.84 Ga (Nozhkin et al., 2003). The second stage of UHT metamorphism was associated with crustal extension and advection of heat through asthenospheric upwelling (1.78–1.73 Ga) (Likhanov et al., 2015c, 2016; Sukhorukov et al., 2018a,b).

Rocks of the Yenisei metamorphic complex form a series of blocks in the zone of the Yenisei fault, extending as a strip in a NW direction for about 170 km, and are separated by a mylonite zone from granulites of the Kan complex (Fig. 2). In addition, these rocks are found in the north of the Angara–Kan block, where they overlie the rocks of the Kan complex. Within the Yenisei fault, the blocks of rocks of the Yenisei complex are divided into a series of tectonic sheets differing in their lithology and structure. Partial sections are exposed on the banks of the Yenisei River, north of the village of Predivinsk. These tectonic sheets underwent heterogeneous metamorphism ranging from epidote-amphibolite and to amphibolite facies (Nozhkin et al., 2016). The ob-

served differences in the *P–T* conditions of metamorphism for different rocks (630–770 °C at 7.3–8.5 kbar) may indicate local heating of metabasic rocks during viscous deformation and/or excess tectonic pressure over the lithostatic pressure as a result of dynamic metamorphism along ductile shear zones of the Yenisei complex (Likhanov et al., 2006, 2014, 2015a,b, 2018a), which is in good agreement with the results of numerical simulation (Ten, 1993; Burg and Schmalholz, 2008; Schmalholz and Podladchikov, 2013).

The Yenisei complex is composed of four metamorphic sequences, including amphibolite-marble-paragneiss (volcanic-carbonate-terrigenous), amphibolite-orthogneiss (volcanic), marble-paragneiss (carbonate-terrigenous), and paragneiss (terrigenous) (Nozhkin, 1999; Nozhkin et al., 2016). Sequence I (1000–1600 m) is composed of biotite (±Grt, Sil) gneisses and biotite-quartz schists interbedded with biotite-amphibole plagiogneisses, dolomite marbles, and calciphyres (0.2–1.5 m thick) and contains boudinized layers of amphibolites (metabasites). The rocks are migmatized and intruded by veins of gneissic porphyritic and leucocratic granites and pegmatites. This sequence is well exposed on the right bank of the Yenisei River from the village of Predivinsk to the mouth of the Posol'naya River. A fragment of this sequence with a similar lithology crops out in the north, on the left bank of the Yenisei River and near the mouth of the Osinovyi Creek. The age of amphibole-biotite plagiogneisses, whose magmatic origin is undoubted, is estimated to be 1.88 Ga based on the U–Pb data on zircon (Bibikova et al., 1993).

Sequence II (~1500 m) is composed of biotite-two-feldspar microgneiss and biotite-quartz-feldspar (±Grt) schist, biotite (±Amph) plagiogneiss, and biotite-amphibole-feldspar schist and plagioclase amphibole (Nozhkin, 1999; Nozhkin et al., 2016). The REE and trace element systematics of metavolcanics provide grounds to combine these rocks into three associations: andesite–dacite–trachyrhyodacite, leucobasalt–basalt, and basalt–andesibasalt–trachyandesite. Sequence II is best exposed along the left bank of the Yenisei River between the Kalinkin and Lugovskoi Creeks. The U–Pb dating of zircons from two samples of metavolcanic andesite-dacite-trachyrhyodacite association established that volcanics formed in the late Paleoproterozoic (~1.74 Ga) and underwent metamorphism at 750 Ga (Nozhkin et al., 2016).

Sequence III (1500–2000 m) is composed mainly of biotite and two-mica (±Grt) gneisses, mica-quartz schists intercalated with feldspar quartzites and layers (3–5 to 50 m thick) of calcite and dolomite marbles. This sequence crops out in natural cliffs on the left bank of the Yenisei River, some 3.5–2 km upstream from the Zaliv floodplain. The biotite gneisses are mylonitized and pass into thinly banded chlorite-mica-feldspar-quartz (±Grt) schists with lenses of granular aggregates of quartz or quartz-feldspar.

Paragneiss Sequence IV (not less than 2000 m thick) is composed mainly of compositionally homogeneous two-mica muscovite-biotite and chlorite-muscovite-biotite plagiogneisses, containing a few horizons of two-feldspar muscovite-biotite (±Chl) gneisses and garnet-sillimanite-mica schists, as well as layers of mica-feldspar quartzites. In places, the layers have a fine banding due to weak migmatization/K-feldspathization. Dikes of amphibolized basic rocks are present locally. This sequence is best exposed on the left bank of the Yenisei River between Shivera and Atamanovo Villages.

The Taraka granitoid pluton in the northeast of the Angara–Kan block intrudes the Kan granulite complex and is comprised of three spatially associated granitoids suites of different ages. The first suite occurring in the western boundary zone is composed of gneissic garnet- and cordierite-containing granites and plagiogranites. Syntectonic granites are classified as S-type granites (Nozhkin et al., 2003) that appear to be almost synchronous with the high-T metamorphic event. The second suite makes up the bulk of the massif and is represented by porphyritic biotite granites and A-type leucogranites (Nozhkin et al., 2003). These granites, interpreted as posttectonic, were emplaced at 1837 ± 3 Ma. The third suite, developed in the northern part of the pluton, is comprised of porphyritic biotite granites and leucogranites with large (up to 2 × 5 cm) tabular crystals of K-feldspar. These Fe–K subalkaline granites have enriched radioactive and trace element concentrations (in ppm): U = 6–8, Th = 80–100, Zr = 460–470, La = 80–150, Y = 25–80, and are classified as A-type granites. Based on a U–Pb zircon age of 1746 ± 3 Ma, they were emplaced during and intraplate tectonic event (Nozhkin et al., 2009).

ANALYTICAL TECHNIQUES

Major and trace elements. Major oxide and trace element analyses were performed at the Analytical Center of V.S. Sobolev Institute of Geology and Mineralogy, Siberian Branch, Russian Academy of Sciences, Novosibirsk. Major element data were obtained by XRD (analysts N.M. Glukhov and N.G. Karmanova) and trace elements were determined using a Finnigan Mat ELEMENT high-resolution inductively coupled plasma mass spectrometer (ICP–MS) equipped with a U-5000AT+ ultrasonic nebulizer, following the procedures described in (Nikolaeva et al., 2008). The precision of the data does not exceed 2–7% rel. REE and trace elements were analyzed in some samples by instrumental neutron activation (analyst V.S. Parkhomenko). The differences between the concentrations of elements analyzed by different techniques in the same samples were within acceptable ranges.

Sm–Nd isotopy. Sm and Nd isotopic measurements were performed at the Geological Institute of the Kola Scientific Center, Russian Academy of Sciences, Apatity (analyst P.A. Serov), following the procedures described in (Bayanova, 2004).

U–Pb dating. Zircons were separated for U–Pb dating at the Analytical Center of the IGM SB RAS using a common method of heavy liquids and magnetic separation. Zircon

grains were handpicked under a binocular microscope. Zircon crystal morphology and internal structures were examined under transmitted and reflected light. The internal structures of zircons were documented by cathodoluminescence imaging.

U–Pb dating of zircons from granite was carried out with a SHRIMP-II ion microprobe at the Center for Isotopic Research (VSEGEI, St. Petersburg, analyst A. Larionov), following the standard procedure (Williams et al., 1998; Schuth et al., 2012). Cathodoluminescence, transmitted and reflected light images showing the internal structure and zoning patterns of zircons were used to guide the selection of analysis points. The primary molecular oxygen beam was optimized to a current of 4 nA with a dimeter of 25 μm and a depth of 2 μm. The data were processed using the SQUID software (Ludwig, 2000). The U/Pb ratios were normalized to a value of 0.0668 for the TEMORA standard zircon corresponding to an age of 416.75 Ma. All errors for ratios and ages are 1σ, and those for the calculated concordant and intercept ages are 2σ. Concordia plots were constructed using the ISOPLOT/EX software (Ludwig, 1999).

U–Pb isotope dating of detrital zircons was performed by laser ablation-inductively coupled plasma mass spectrometry (LA-ICP-MS, Nu Instruments) equipped with a Resonetics RESOlution M-50-HR Excimer Laser Ablation System at the Department of Earth Sciences of the University of Hong Kong. The zircon 91500 reference material was used as an external standard for U–Pb dating. The analytical procedures were described in detail by Xia et al. (2011). Measured values were processed using the ICPMSDataCal (Liu et al., 2010) and Isoplot/Ex v.3. softwares (Ludwig, 2003). All errors for ratios and ages are ±1σ. The U–Pb ages reported in this study are $^{206}Pb/^{207}Pb$ ages for grains older than 1 Ga, and $^{206}Pb/^{238}U$ ages for younger grains. The diagrams were constructed using the Isoplot 4.0 software. Analyses showing ≤5% discordance were used.

LITHOGEOCHEMICAL CHARACTERISTICS OF SCHISTS AND GNEISSES OF THE YENISEI METAMORPHIC COMPLEX

The mineral and chemical composition of representative metasedimentary rock samples from three sequences are shown in Tables 1–4.

Major oxides. Based on the systematics of the reconstruction of protoliths of metasedimentary rocks (Neelov, 1980), the gneisses and schists of amphibolite-marble-paragneiss Sequence I correspond to two groups of rocks: polymictic sandstone and siltstone-mudstone. Two-mica and garnet–two-mica schists of marble-paragneiss Sequence III mostly correspond to mudstones and their carbonaceous varieties, and the biotite and two-mica gneisses of paragneiss Sequence IV range from arkose sandstones and siltstones to mudstones. The rocks of Sequence III are characterized by the lowest SiO_2 (58.8%), highest Al_2O_3 (19.1%), and moderate Fe_2O_3 (9.2%) and K_2O (4.0%) concentrations. The paragneisses of sequences I and IV have almost similar average compositions and differ in their low Al_2O_3 (14.2 and 14.8%), Fe_2O_3, TiO_2 and K_2O contents and generally higher SiO_2 (64.8–67.7%). The difference between these sequences is that the latter forms an almost continuous rock series characterized by a decrease in Al_2O_3 and Fe_2O_3 and an increase in SiO_2, while the rocks of Sequence I can be classified into two distinct groups with low and high SiO_2 contents (60–63% and 71–73%) and, respectively, with high and low Al_2O_3, Fe_2O_3 and TiO_2. Rocks of Sequences I and IV display the lowest chemical index of alteration (CIA): 56–66 and 58–68. Based on their CIA values, the metapelites of Sequence III (66–79) correspond to products of intensive chemical weathering.

At the same time, the presence of significant correlation between the major petrochemical modules (FM, IM, TM) (Yudovich and Ketris, 2000) indicates that the protoliths of the Yenisei complex are the first-cycle sediments. The effects of recycling are documented only in the rocks of Sequence III, mostly mudstones, and do not generally exhibit an inverse correlation between the femic (FM) and sodium-potassium (SPM) modules typical of petrogenic sediments (Yudovich and Ketris, 2000).

Trace and rare earth elements. All studied samples of metasedimentary rocks of the Yenisei complex (Fig. 3, Tables 2–4) exhibit a pronounced negative Eu anomaly, the average Eu/Eu* (about 0.6) are similar to the average PAAS, which indicates the presence of rocks of high-K felsic magmatic series in the source area. The total REE content of gneisses and schists from sequences I and IV is 1.2–1.3 times higher than the average PAAS, and reaches the highest value in the third strata of rocks. The average $(La/Yb)_n$ values of rocks from different sequences are similar to each other (11.4–13.4) and are generally higher than those for PAAS. Strong variations in the heavy REE content of the studied rocks can be associated with an uneven distribution of garnet, the main concentrator of these elements.

Gneisses and schists in all sequences have high (average 19–22 ppm) Th content, which is 1.4 times higher than that of the average PAAS. The average concentrations of Zr, Hf, Y, and Sc are close to, while U and Sr are lower than those of the PAAS. The rocks of Sequences I and IV have almost similar concentrations of most of the trace elements, while the metapelites of Sequence III show enrichment not only in K, Rb, and Th, but also in HFSE, REE and Fe, Cr, Ni, and Co. Such compositional variations observed in Sequence II can be explained are due to the increased content of clay-sized fractions in the initial sediments, which tend to concentrate most of the trace elements (Taylor and McLennan, 1988).

Given the petrogenic nature of the sedimentary protoliths for the Yenisei complex, as indicated by the abnormally low Cr/Th (2.0–8.3) and high La/Sc (1.4–4.5) ratios and the presence of a distinct Eu minimum, we can assume a sharp dominance of felsic rocks in the source areas. One of the

Table 1. Mineral assemblages from analyzed paragneisses, crystalline schists (metapelites) and marbles of the Yenisei complex

No.	Sample No.	Rock	Mineral assemblage	Sampling site
Amphibolite-marble-paragneiss sequence				
1	237-78	Two-mica schist	Ms + Bt + Pl + Qtz	Right bank of the Yenisei River, cliff outcrops, from Predivinsk Village to Srednii Creek
2	244-78	Biotite-amphibole plagiogneiss	Bt + Amph + Pl + Qtz	
3	253-78	Garnet-biotite gneiss	Grt + Bt + Pl + Qtz	
4	255-78	Garnet-biotite gneiss	Grt + Bt + Pl + Qtz	
5	263-78	Biotite gneiss	Bt + Kfs + Pl + Qtz	
6	242-78	Biotite gneiss	Bt + Kfs + Pl + Qtz	
7	262-78	Dolomite marble	Cal + Dol + Amph + Scp	
8	283-78	Sillimanite-garnet-biotite gneiss	Sil + Grt + Bt + Pl + Qtz	Right bank of the Yenisei River, cliff outcrops, from Srednii Creek to Posol'naya River mouth
9	274-78	Garnet-biotite gneiss	Sil + Grt + Bt + Pl + Qtz	
10	273-78	Garnet-two-mica gneiss	Grt + Ms + Bt + Chl + Pl + Qtz	
11	281-78	Biotite gneiss	Bt + Pl + Qtz	
Marble-paragneiss sequence				
1	200-79	Two-mica schist	Bt + Ms + Pl + Qtz	Left bank of the Yenisei River, cliff outcrops, 3.5–2 km upstream from the Zaliv floodplain
2	205-79	Garnet-two-mica gneiss, cataclastic	Grt + Bt + Ms + Pl + Qtz	
3	207-79	Mylonite after biotite gneiss	Grt + Bt + Ms + Chl + Pl + Qtz + Hem	
4	203-79	Two-mica schist, mylonitized	Bt + Ms + Pl + Qtz	
5	208-79	Dolomite marble	Cal + Dol + Amph + Scp	
6	209-79	Calciphyre	Cal + Cpxl + Amph + Ves + Scp	
Paragneiss sequence				
1	1-85	Biotite gneiss	Bt + Kfs + Pl + Qtz	Yenisei River, cliff outcrops, from Shivera Village to Atamanovo Village
2	2a-85	Biotite plagiogneiss	Bt + Pl + Qtz	
3	1-12	Biotite plagiogneiss	Bt + Pl + Qtz	
4	6-12	Biotite gneiss	Bt + Kfs + Pl + Qtz	
5	260-79	Biotite-muscovite gneiss	Bt + Ms + Kfs + Pl + Qtz	
6	262-79	Biotite-muscovite gneiss	Bt + Ms + Chl + Pl + Qtz	
7	266-79	Biotite-muscovite plagiogneiss	Bt + Ms + Pl + Qtz	
8	269-79	Biotite gneiss	Bt + Ms + Kfs + Pl + Qtz	
9	274-79	Garnet-two-mica gneiss	Grt + Bt + Ms + Kfs + Pl + Qtz	
10	277-79	Biotite-muscovite plagiogneiss	Bt + Ms + Pl + Qtz	

Note. Ms, muscovite; Bt, biotite; Pl, plagioclase; Qtz, quartz; Amph, amphibole; Grt, garnet; Kfs, K-feldspar; Sil, sillimanite; Hem, hematite; Chl, chlorite; Cal, calcite; Dol, dolomite; Cpx, clinopyroxene; Scp, scapolite; Ves, vesuvian.

main sources of terrigenous material could be rocks of the Kan charnockite-granulite complex, which is laterally associated with the Yenisei complex in the structure of the Angara–Kan block. To test this assumption, we compare the average compositions of rock samples from sequences I and IV and the third layer of the Yenisei complex with the average compositions of the Kan rocks using the data of Nozhkin and Turkina (1993). This comparison shows that the rock samples from Sequences I and IV display a 10–20% difference in the concentrations of most components as compared to the rocks of the Kan complex, whereas rocks of Sequence III are more enriched in trace elements (up to 20–60%) due to the presence of pelitic sediment (Fig. 4). In addition, the rocks of the Yenisei complex show a 20% depletion in Eu relative to the Kan granulites. The overall similarity of the average trace element concentrations in the rocks of these two complexes suggests that the composition of the Kan granulites was inherited by metasedimentary rocks of the Yenisei complex, while the U and Rb concentrations here are 2.3 and 1.4–2.3 times higher, respectively. Higher concentrations of U and Rb in schists and gneisses are consistent with their lower metamorphic grade compared to the Kan rocks, which became depleted in these elements during granulite-facies metamorphism (Nozhkin and Turkina, 1993). Note that higher Th concentrations and pronounced negative deeper Eu anomalies in metasedimentary rocks of the Yenisei complex are explained by the presence of K-rich granitoids in their source area, which were emplaced at the final stage of the formation of the Kan charnockite-granulite complex.

Table 2. Major oxide (wt.%) and trace element (ppm) contents of representative samples of metapelites and marbles from the amphibolite-marble-paragneiss sequence, Yenisei complex

Component	1	2	3	5	6	7	8	9	10	11
	237-78	244-78	253-78	263-78	262-78	242-78	283-78	274-78	273-78	281-78
SiO_2	63.16	59.69	66.02	61.00	10.62	62.91	61.30	70.96	71.25	73.31
TiO_2	0.61	1.08	0.56	0.96	0.16	0.85	0.83	0.56	0.61	0.49
Al_2O_3	14.58	15.29	13.27	16.90	2.04	15.34	16.93	13.80	13.69	12.51
Fe_2O_3	6.38	8.93	6.79	8.33	1.50	6.81	8.78	4.76	5.16	3.82
MnO	0.12	0.12	0.16	0.13	0.08	0.15	0.08	0.05	0.07	0.07
MgO	3.06	4.00	4.14	3.35	16.59	2.70	3.37	2.32	0.71	0.91
CaO	5.18	4.77	6.16	4.10	32.68	3.54	1.76	1.54	1.68	2.95
Na_2O	2.39	2.54	0.48	0.72	0.10	3.52	2.77	1.87	2.49	2.87
K_2O	2.57	2.40	1.30	3.43	0.26	2.56	3.05	3.21	2.89	1.99
P_2O_5	0.15	0.16	0.15	0.16	0.03	0.24	0.18	0.15	0.18	0.21
LOI	1.95	1.54	1.56	1.35	36.45	1.51	1.16	0.64	1.37	0.62
Total	99.73	99.88	100.15	99.73	100.43	99.64	99.49	99.51	99.73	99.54
Th	21.0	17.4	10.9	18.2	1.0	22.4	17.4	35.0	25.0	14.5
U	1.6	1.1	2.5	3.7	0.9	2.4	3.0	6.4	2.5	2.4
Rb	105	100	69	191	8	118	150	128	184	92
Ba	369	518	396	405	45	570	640	850	907	408
Sr	197	150	92	78	115	200	130	170	195	153
La	41	45	31	40	4.8	37	43	97	67	39
Ce	72	90	73	82	10.3	74	93	198	133	74
Pr	7.6	10.3	7.0	9.5	–	–	–	–	14.0	8.5
Nd	25	37	27	35	5.5	33	41	86	48	31
Sm	4.4	7.0	5.5	6.4	1.3	6.6	7.0	16.4	9.4	5.3
Eu	1.0	1.5	1.2	1.4	0.2	1.2	1.3	1.7	1.9	1.2
Gd	3.8	6.0	5.1	5.7	1.4	5.8	3.6	12.9	8.1	4.8
Tb	0.6	0.9	0.8	1.0	0.2	0.9	0.9	1.8	1.0	0.7
Dy	3.0	5.1	4.7	5.8	–	–	–	–	4.4	3.6
Ho	0.6	1.1	1.0	1.3	–	–	–	–	0.8	0.8
Er	1.8	3.0	2.7	4.0	–	–	–	–	1.6	2.2
Tm	0.3	0.5	0.4	0.6	0.1	0.4	0.5	0.8	0.2	0.3
Yb	1.8	2.9	2.7	4.2	0.6	2.7	2.9	5.0	1.3	2.2
Lu	0.3	0.4	0.4	0.6	0.1	0.4	0.4	0.8	0.2	0.1
Zr	171	264	120	238	54	230	210	310	107	210
Hf	4.9	7.6	3.6	6.6	1.3	5.2	4.6	15.4	2.7	5.8
Nb	6.7	11.1	11.1	14.6	–	–	–	–	17.0	9.0
Ta	0.4	0.7	0.9	1.2	0.2	0.8	1.1	1.7	0.8	0.9
Y	17.8	29	28	36	–	–	–	–	19	22
Cr	61	68	65	71	8	70	80	28	85	82
Ni	37	10	40	45	5	10	34	15	30	37
Co	25	26	24	21	2	26	16	10	14	16
V	164	100	130	109	33	90	108	50	84	99
Sc	24	22	22	21	2	22	23	11	15	18
$(La/Yb)_n$	15.1	10.5	7.7	6.4	5.5	9.4	10.0	13.0	35.0	12.0
Eu/Eu*	0.7	0.7	0.7	0.7	–	0.6	0.7	0.3	0.6	0.7
Cr/Th	2.9	3.9	6.0	3.9	–	3.1	4.6	0.8	3.4	5.7
La/Sc	1.7	2.0	1.4	1.9	–	1.7	1.9	8.8	4.5	2.2

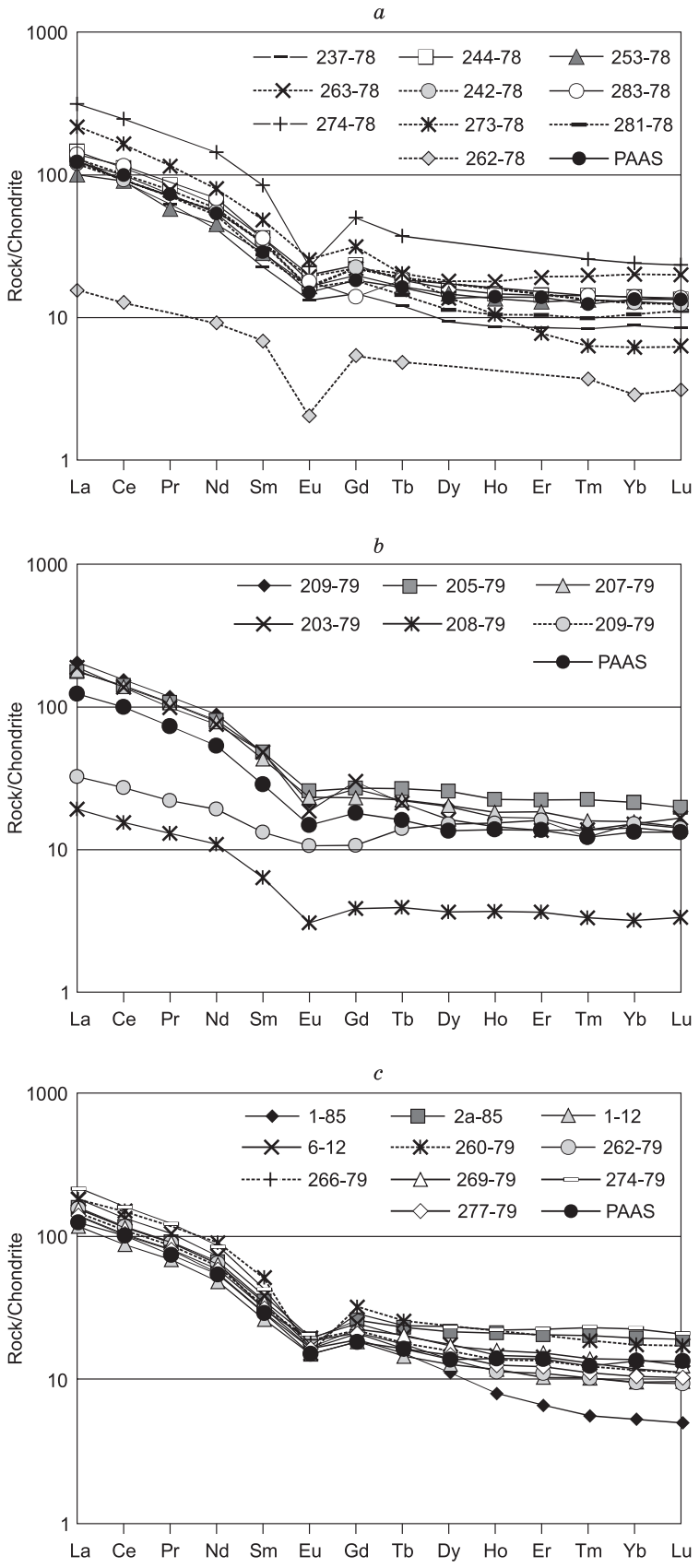

Fig. 3. REE patterns for metasedimentary rocks of the Yenisei complex. Sequences: I (*a*), III (*b*), IV (*c*). Sample numbers are the same as in Tables 2–4.

Table 3. Major oxide (wt.%) and trace element (ppm) contents of representative samples of metapelites and metacarbonate rocks from the marble-paragneiss sequence, Yenisei complex

Component	1	2	3	4	5	6
	200-79	205-79	207-79	203-79	208-79	209-79
SiO_2	56.85	58.29	59.22	61	17.62	54.51
TiO_2	0.95	1.29	0.85	0.96	0.16	0.71
Al_2O_3	20.57	19.36	19.57	16.9	2.4	13.61
Fe_2O_3	9.29	10.62	8.49	8.33	1.06	8.32
MnO	0.14	0.18	0.11	0.13	0.01	0.09
MgO	2.49	2.02	2.2	3.35	13.63	6.55
CaO	0.3	0.87	0.28	4.1	33.34	9.35
Na_2O	0.37	1.1	0.22	0.42	0.08	1.43
K_2O	4.55	3.69	4.26	3.43	0.69	2.04
P_2O_5	0.08	0.16	0.08	0.07	0.05	0.06
LOI	4.45	2.41	4.42	1.35	30.68	3.31
Total	100.04	99.99	99.7	99.64	99.72	99.96
Th	22	21	20	23.3	2.5	6.5
U	2.7	3.2	2.1	2.6	2.8	7.8
Rb	280	208	243	192	37	101
Ba	537	643	641	498	91	321
Sr	75	147	73	34	581	488
La	63	54	55	58	6	10.1
Ce	124	113	111	110	12.6	22
Pr	14.3	13	12.9	12	1.6	2.7
Nd	53	48	47	45	6.6	11.6
Sm	9.3	9.4	8.4	9.4	1.26	2.6
Eu	1.59	1.9	1.72	1.38	0.23	0.79
Gd	6.9	7	6	7.8	1.02	2.8
Tb	1.05	1.27	1.06	1.01	0.19	0.67
Dy	6.5	8.3	6.6	5.27	1.2	4.9
Ho	1.22	1.62	1.32	1.05	0.27	1.11
Er	3.5	4.7	3.9	2.89	0.78	3.4
Tm	0.45	0.73	0.52	0.45	0.11	0.4
Yb	3	4.5	3.3	3.19	0.68	3.2
Lu	0.43	0.64	0.47	0.54	0.11	0.46
Zr	265	271	224	132	54	127
Hf	5.4	5.2	1.4	3.6	1.01	2.7
Nb	25	28	22	20	3.4	8.1
Ta	1.28	1.5	1.2	1.29	0.15	0.57
Y	38	53	41	26	8.9	36
Cr	91	150	103	118	14	140
Ni	50	98	98	43	28	170
Co	28	41	31	22	5.3	40
V	125	176	108	116	108	216
Sc	21	18	20	22.5	23	25
$(La/Yb)_n$	14.2	8.1	11.2	12.3	5.9	2.1
Eu/Eu*	0.6	0.7	0.7	0.5	0.6	0.9
Cr/Th	4.1	7.1	5.2	5.1	–	–
La/Sc	3.0	3.0	2.8	2.6	–	–

GEOCHRONOLOGICAL RESULTS

U–Pb dating of zircons from granites. The age of Sequence I (amphibolite-marble-paragneiss) was determined on a granite vein cutting through it. On the right bank of the Yenisei River, 2 km upstream from the mouth of the Posol'naya River, the migmatized garnet-biotite gneisses are cut by a thick (15–20 m) body of pink-gray porphyritic granites. The gneissic biotite granites contain garnet and numerous (25–30 vol.%), subparallel-oriented phenocrysts of K-feldspar and, more rarely, felsic plagioclase, ranging from 2 to 8 mm in size. The groundmass is fine-grained (0.1–0.3 mm), and composed of quartz-feldspar with minor biotite (up to 5%) and accessory zircon and apatite. Gneissic granites are cut by small veins of pegmatoid granites and medium-grained leucogranites and show aureoles of muscovitization at contacts with the latter. Compositionally, these granites are subalkaline, peraluminous (ASI = 1.2), high-K ($K_2O + Na_2O = 8.53\%$, $K_2O/Na_2O = 2.5$), enriched in Rb, Ba, and LREE (Table 5). They are characterized by low HREE and high $(La/Yb)_n$ values, and a pronounced negative Eu anomaly (Eu/Eu* = 0.47). Based on their high Th contents (41–50 ppm), these granites are similar to subalkaline granites of the Taraka pluton (Nozhkin et al., 2003; Nozhkin and Rikhvanov, 2014).

Zircons from granite have prismatic to bipyramidal morphology, grain size of 150-400 μm, and aspect ratio of 2.5–5 (Fig. 5). The grains are transparent, light yellow in color. In cathodoluminescence (CL) images, most of the grains display thin oscillatory zoning, some grains display a bipyramidal-prismatic core and a dark rim. The discordia line constructed on 14 analysis points defines an upper concordia intercept at 1844 ± 8 Ma (MSWD = 1.14) (Fig. 6*a*), with a weighted mean of 1847 ± 5 Ma (MSWD = 1.03) (Fig. 6*b*). Two cores yielded $^{206}Pb/^{207}Pb$ ages of 2526 ± 8 and 2762 ± 16 Ma (late Archean), suggesting that they could be inherited from the source of granites (Table 6). The age of the

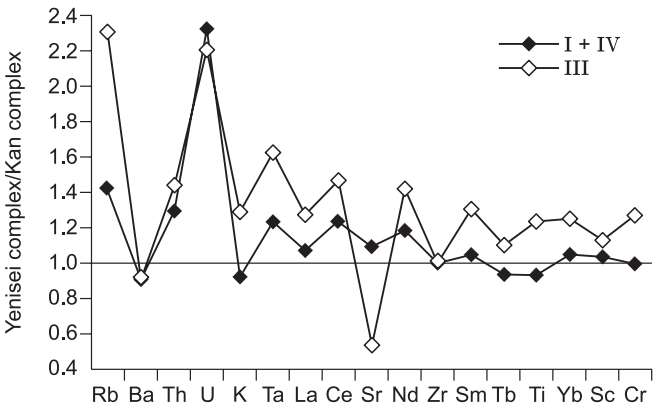

Fig. 4. Multielement patterns for rocks of the Yenisei complex. Average composition: I + IV, samples collected of sequences I and IV; III, Sequence III. Normalized to the average compositions of granulites of the Kan complex (Nozhkin and Turkina, 1993).

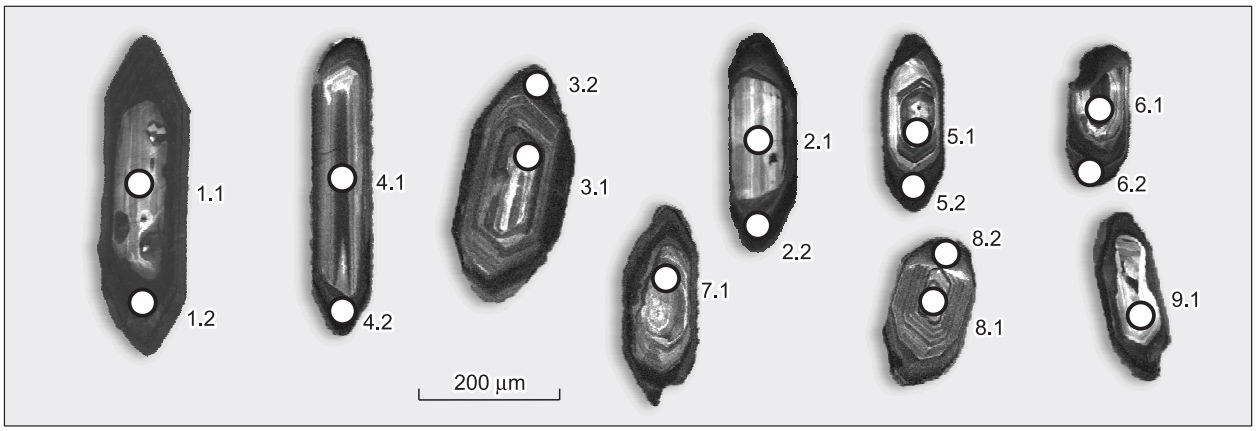

Fig. 5. Cathodoluminescence image of zircons from granites cutting Sequence I of the Yenisei complex with position of analytical spots from Table 2.

granite vein is interpreted to close to the emplacement age of subalkaline granites of the Taraka pluton (1837±3 Ma) (Nozhkin et al., 2003). These granites were formed from a crustal source with a late Archean model age $T_{Nd}(DM)$ = 2.7 Ga and ε_{Nd} = –5.6 (Table 7), which is consistent with the presence of Neoarchean zircon cores in these granites. The age of the granitic intrusions suggests that the upper boundary of Sequence I is not younger than 1.85 Ga.

LA-ICP-MS dating of detrital zircons. Detrital zircons from metasedimentary rocks were used for age determination and provenance studies. A biotite plagiogneiss (sample A-50-12) with Bt + Pl + Qtz and accessory sphene, apatite, and zircon was collected on the right bank of the Yenisei River, 0.6 km downstream of Predivinsk (57°05′33″ N, 93°27′35″ E) from a member of migmatized biotite and biotite-amphibole gneisses, containing the boudinaged garnet amphibolites. This member is part of the amphibolite-marble-paragneiss sequence of the Yenisei complex. Garnet amphibolites formed under upper amphibolite facies metamorphic conditions (760–820 °C and 8.0–9.7 kbar). Sixty-one zircons were >95% concordant out of 91 zircon grains extracted from this sample for analysis. All zircon grains analyzed in this sample belong to two populations. About 35% zircons are light-colored, translucent, prismatic or, more rarely, bipyramidal to prismatic grains, with smoothed edges and terminations, 100–250 μm in size and aspect ratio of 1.5–2.5. Most of the zircons (~65%) are transparent, rounded, isometric, light brown or colorless.

All zircons in this sample are Paleoproterozoic in age (Fig. 7*a*). The most abundant zircon population is of late Paleoproterozoic age. Most of these grains yielded a $^{206}Pb/^{207}Pb$ age of 1.77–1.93 Ga with a major peak on the probability plot at 1.84 Ga. The older Paleoproterozoic zircon population (2.2–2.4 Ga) is represented by 7 grains (12%), the youngest population of at least two grains gave ages of 1754 ± 10 and 1755 ± 5 Ma.

All these age values resulted from CL-dark, unzoned zircons and, more rarely, zircon rims. This evidence suggests that these grains have suffered significant alteration (me-

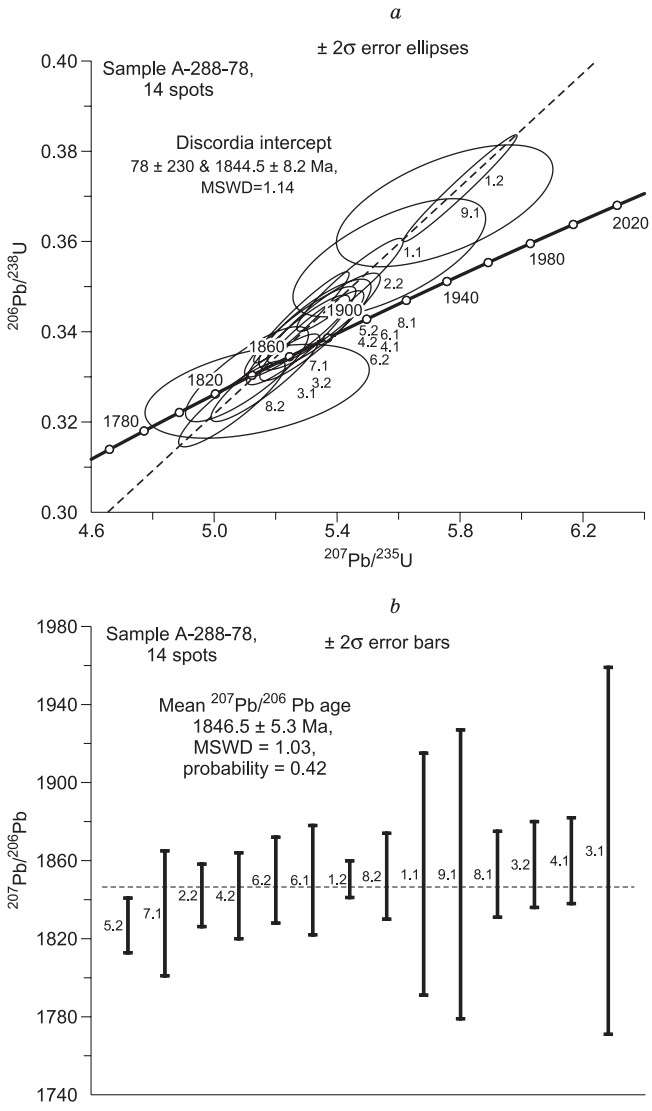

Fig. 6. Concordia plot of zircons from granites cutting Sequence I of the Yenisei complex (*a*) and the distribution of the $^{207}Pb/^{206}Pb$ ages for the same zircons (sample A-288-78) (*b*). The numbers of analysis points are the same as in Table 1.

Table 4. Major oxide (wt.%) and trace element (ppm) contents of representative samples of metapelites from the paragneiss sequence, Yenisei complex

Component	1	2	3	4	5	6	7	8	9	10
	1-85	2a-85	1-12	6-12	260-79	262-79	266-79	269-79	274-79	277-79
SiO_2	69.61	63.54	70.92	68.06	72.30	58.83	67.79	70.56	66.00	69.68
TiO_2	0.57	0.74	0.60	0.84	0.48	0.89	0.71	0.62	0.59	0.66
Al_2O_3	13.29	16.07	13.14	13.41	12.60	17.10	13.89	13.04	15.60	13.44
Fe_2O_3	5.93	8.38	5.38	6.48	4.64	10.07	7.13	5.46	8.59	5.79
MnO	0.05	0.15	0.06	0.09	0.06	0.10	0.11	0.06	0.30	0.06
MgO	1.56	2.34	1.68	2.27	2.30	3.22	2.59	1.72	1.65	1.79
CaO	2.36	3.40	2.78	1.78	1.25	2.85	1.94	2.47	0.85	2.63
Na_2O	2.70	2.79	2.90	2.28	1.72	2.60	2.27	2.39	1.63	3.19
K_2O	2.93	2.45	1.84	3.85	2.74	2.61	2.52	2.99	3.64	1.94
P_2O_5	0.09	0.16	0.12	0.12	0.12	0.09	0.19	0.11	0.11	0.11
LOI	0.24	0.19	0.52	0.69	1.96	1.41	1.41	0.52	1.69	0.59
Total	99.49	100.4	100.0	100.0	100.2	99.88	100.2	100.4	99.97	99.96
Th	16.6	17.6	13.9	23	23.0	21	17.6	18.0	27	17.2
U	1.85	2.3	2.3	2.7	2.1	1.48	1.79	2.5	3.1	1.75
Rb	118	151	100	135	75	124	139	124	145	108
Ba	522	480	320	882	830	603	447	606	1 130	363
Sr	147	150	262	211	184	204	145	214	137	175
La	42	48	36	56	55.0	47	45	47	66	42
Ce	81	93	69	106	119.0	92	87	91	127	82
Pr	9.6	10.9	8.2	12.5		10.7	10.3	10.9	14.7	9.7
Nd	33	39	29	43	53.0	38	36	38	51	35
Sm	5.6	6.8	5.1	7.4	9.9	6.0	6.1	6.6	8.2	6.1
Eu	1.20	1.40	1.09	1.42	1.1	1.35	1.38	1.23	1.26	1.20
Gd	4.9	6.7	4.7	6.3	8.2	5.4	5.7	5.7	7.4	5.4
Tb	0.71	1.08	0.68	0.94	1.2	0.83	0.84	0.96	1.11	0.77
Dy	3.6	6.9	4.1	5.6	–	4.4	5.1	5.5	7.5	4.7
Ho	0.57	1.50	0.84	1.05	–	0.81	0.98	1.14	1.57	0.90
Er	1.38	4.3	2.2	3.0	–	2.3	2.8	3.2	4.7	2.6
Tm	0.18	0.65	0.33	0.42	0.6	0.33	0.40	0.45	0.74	0.36
Yb	1.10	4.0	2.0	2.5	3.62	1.98	2.4	2.9	4.7	2.2
Lu	0.16	0.61	0.31	0.36	0.55	0.30	0.36	0.40	0.66	0.33
Zr	214	212	215	320	255	179	210	306	275	251
Hf	5.7	5.8	5.6	8.9	7.3	5.2	5.9	8.3	8.1	6.9
Nb	11.7	14.9	11.8	14.5	14.0	17.1	14.1	14.9	16.1	12.8
Ta	0.79	1.19	0.92	0.92	0.75	1.06	0.91	0.95	0.86	0.79
Y	19.0	44	25	32	30.0	24	30	33	46	27
Cr	138	109	90	190	45	106	86	59	58	71
Ni	38	40	66	142	20	62	51	27	18.7	39
Co	15.1	20	15.1	19.1	9	25	21	13.0	15.8	15.7
V	82	119	84	113	60	140	110	78	74	88
Sc	10.0	24	13.4	15.3	10	26	17.5	12.3	16.2	14.5
$(La/Yb)_n$	25.7	8.1	12.1	15.2	10.2	16.1	12.5	11.1	9.6	13.1
Eu/Eu*	0.7	0.6	0.7	0.6	0.4	0.7	0.7	0.6	0.5	0.6
Cr/Th	8.3	6.2	6.4	8.4	2.0	5.1	4.9	3.3	2.2	4.1
La/Sc	4.2	2.0	2.7	3.6	5.5	1.8	2.5	3.8	4.1	2.9

Table 5. Major (wt.%) and trace element (ppm) contents of representative samples of granites, Yenisei complex

Component	1	2
	A-288-78	A-287-78
SiO_2	70.40	70.27
TiO_2	0.26	0.24
Al_2O_3	15.06	15.23
Fe_2O_3	0.65	1.04
FeO	1.97	1.93
MnO	0.04	0.06
MgO	0.86	0.20
CaO	1.12	1.96
Na_2O	2.45	2.60
K_2O	6.08	5.11
P_2O_5	0.20	0.16
LOI	0.43	0.82
Total	99.52	99.62
Th	50.0	41.0
U	3.5	3.0
Rb	172	193
Cs	1.1	1.41
Ba	741	722
Sr	178	160
La	72	64
Ce	147	128
Pr	16.2	15
Nd	55	52
Sm	10.6	9.2
Eu	1.1	1.24
Gd	7.8	6.6
Tb	0.99	0.86
Dy	5.6	4.2
Ho	1.02	0.76
Er	2.6	1.83
Tm	0.35	0.24
Yb	1.82	1.38
Lu	0.23	0.19
Y	30	22
Zr	238	206
Hf	6.7	6.2
Ta	0.39	0.32
Nb	6.1	5.8
Sc	12	13
Cr	48	36
Co	6	6
Ni	13	12
$(La/Yb)_n$	31	31
$(La/Sm)_n$	4.4	4.4
Eu/Eu*	3.9	3.9

Note. 1, porphyritic biotite granite; 2, porphyritic muscovite granite.

tamictization) during metamorphism of rocks of this stratum with the presence of a fluid phase in the zone of the Yenisei Fault (Nozhkin et al., 2016). The alteration of zircons during metamorphism is indicated, for example, by the presence of

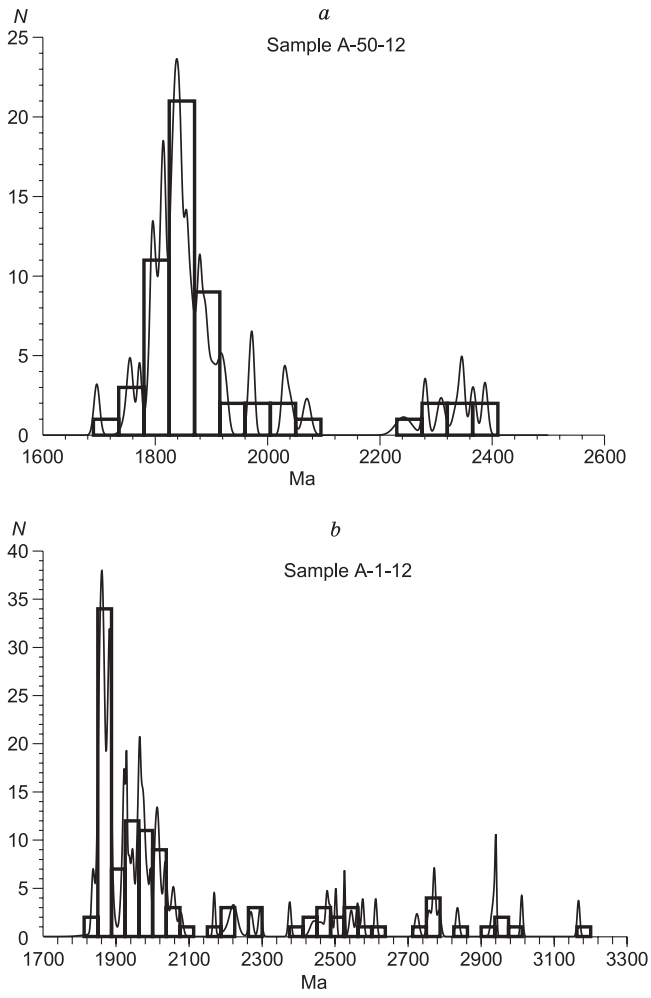

Fig. 7. Frequency histograms and probability density distribution plots curves of $^{207}Pb/^{206}Pb$ ages of zircons from metasedimentary rocks from sequences I (*a*) and IV (*b*). N, number of analyzed zircon grains.

a dark unzoned rim with an age of 1858 Ma on the older (1940 Ma) weakly zoned core. The main peak of ~1.84 Ga, presumably corresponding to the age of alteration coincides with the time of emplacement of subalkaline granitic rocks of the Taraka pluton (Nozhkin et al., 2003) and granitic veins intruding the metasedimentary sequence. The presence of younger (~1.75 Ga) zircons is caused by the second stage of high-temperature metamorphism (~1.77–1.75 Ga) in the Kan granulite complex, which was almost synchronous with the second stage of granite emplacement at the Taraka pluton (Nozhkin et al., 2009; Turkina and Sukhorukov, 2015). Thus, the ages of zircons from granitic veins and detrital zircons provide constraints on the timing of deposition of Sequence I at 1.84 Ga.

A biotite gneiss (sample A-1-12) was collected from Sequence IV (paragneisses) on the left bank of the Yenisei River, 2-3 km downstream from the village of Shivera (56°18′92″ N, 93°32′33″ E). The biotite plagiogneisses (Bt + Pl + Qtz + Zr + Ap) are gray to dark gray, fine-grained rocks. Ninety-five zircons were >95% concordant out of 116 zircon

Table 6. U–Pb isotope data on zircons from the granite (sample A-288-78)

Spot No.	$^{206}Pb_c$, %	U, ppm	Th, ppm	$^{232}Th/^{238}U$	$^{206}Pb^*$, ppm	Isotope ratios								Rho	Age, Ma		*D*, %
						$^{238}U/^{206}Pb^*$	±%	$^{207}Pb/^{206}Pb$	±%	$^{207}Pb^*/^{235}U$	±%	$^{206}Pb^*/^{238}U$	±%		$^{206}Pb/^{238}U$	$^{207}Pb/^{206}Pb$	
5.2	0.01	1173	28	0.02	346	2.914	1.2	0.11167	0.39	5.284	1.2	0.3432	1.2	0.950	1902 ± 19	1827 ± 7	–4
7.1	0.00	208	140	0.70	59.1	3.025	1.3	0.11203	0.87	5.107	1.6	0.3306	1.3	0.826	1841 ± 21	1833 ± 16	0
2.2	0.06	943	52	0.06	284	2.853	1.2	0.11263	0.44	5.442	1.3	0.3504	1.2	0.935	1937 ± 20	1842 ± 8	–5
4.2	0.01	439	93	0.22	128	2.941	1.2	0.11264	0.6	5.28	1.4	0.34	1.2	0.900	1887 ± 20	1842 ± 11	–2
6.2	0.15	576	135	0.24	168	2.956	1.2	0.11309	0.58	5.273	1.3	0.3382	1.2	0.898	1878 ± 19	1850 ± 11	–1
6.1	0.24	473	218	0.48	139	2.926	1.2	0.11312	0.8	5.328	1.4	0.3416	1.2	0.833	1894 ± 20	1850 ± 14	–2
1.2	0.02	2256	66	0.03	721	2.689	1.3	0.11314	0.26	5.801	1.3	0.3718	1.3	0.980	2038 ± 23	18515 ± 5	–9
8.2	0.05	438	145	0.34	122	3.086	1.2	0.11321	0.64	5.058	1.4	0.324	1.2	0.890	1809 ± 20	1852 ± 11	2
1.1	0.23	80	90	1.17	24.5	2.804	1.5	0.1133	1.7	5.57	2.3	0.3564	1.5	0.663	1965 ± 26	1853 ± 31	–6
9.1	0.32	77	72	0.97	24.5	2.716	1.5	0.1133	2	5.75	2.5	0.3679	1.5	0.598	2019 ± 26	1853 ± 37	–8
8.1	0.11	472	222	0.49	139	2.916	1.2	0.11331	0.62	5.357	1.4	0.3429	1.2	0.888	1901 ± 20	1853 ± 11	–3
3.2	0.06	517	188	0.38	147	3.031	1.2	0.11362	0.58	5.167	1.4	0.3298	1.2	0.903	1838 ± 20	1858 ± 11	1
4.1	0.04	460	348	0.78	134	2.949	1.2	0.11374	0.58	5.318	1.3	0.3391	1.2	0.900	1882 ± 20	1860 ± 11	–1
3.1	0.71	234	109	0.48	66.3	3.055	1.3	0.114	2.6	5.14	2.9	0.3268	1.3	0.459	1823 ± 21	1865 ± 47	2
5.1	0.04	375	386	1.06	158	2.045	1.2	0.16679	0.49	11.25	1.3	0.489	1.2	0.932	2566 ± 26	2526 ± 8	–2
2.1	0.05	71	31	0.45	34.1	1.8	1.6	0.1923	0.98	14.73	1.9	0.5554	1.6	0.851	2847 ± 36	2762 ± 16	–3

Note. The errors are within 1σ. Pb_c and Pb* are the portions of common and radiogenic Pb, respectively. The correction for common Pb was made using measured ^{204}Pb. *D*, Discordance $100\cdot((^{207}Pb/^{206}Pb\ age)/(^{206}Pb/^{238}U\ age)$. Rho, Correlation coefficient of the ratios $^{207}Pb^*/^{235}U$ and $^{206}Pb^*/^{238}U$.

grains extracted from this sample for analysis. These zircons are of mostly Paleoproterozoic age (80%). A weighted mean age of the 37 youngest zircons, corresponding to the major peak on the probability plot is 1860 Ma. The presence of oscillatory zoned grains with their high Th/U ratios (0.4–0.9) is indicative of a magmatic source of corresponding age. The age of twenty-eight grains falls in the age range of 1.9–2.0 Ma with peaks at 1925 and 1964 Ma on the probability plot. The remaining zircons yielded a wide age range between ~2.0 and ~3.2 Ga. They show oscillatory zoning and Th/U ratio typical of magmatic zircons. The age of detrital zircons indicates Mesoarchean to Paleoproterozoic sedimentary sources, the latter being predominant. Two CL-dark grains that might have undergone alteration during metamorphism yielded the youngest ages of 1835 and 1839 Ma.

Sm–Nd ISOTOPIC CHARACTERISTICS

The $^{147}Sm/^{144}Nd$ values (0.10–0.13) of the analyzed metavolcanic-terrigenous rocks from different sequences comprising the Yenisei metamorphic complex are close to the average crustal ratio of 0.12 (Table 7), which allows us to use a single-stage $T_{Nd}(DM)$ model age to determine the average age of metaterrigenous sources. The ε_{Nd} values were calculated for the age of the corresponding sequences, which was determined from geochronological data. The $T_{Nd}(DM)$ values for metasedimentary and metavolcanic rocks from sequences I, II, and IV are almost identical and scatter between 2.4 and 2.5 Ga, the ε_{Nd} values range from –4.5 to –1.9. The only exception is the two-mica schist sample from marble-paragneiss Sequence III, which has $T_{Nd}(DM)$ = 2.1 Ga and ε_{Nd} = 0. These data are consistent with dominantly Neoarchean crust in the source area with a minor Paleoproterozoic provenance.

DISCUSSION

Age of volcanosedimentary rocks. Geochronological and isotopic data on zircons from granitic veins (1845 Ma) cutting the gneisses of amphibolite-marble-paragneiss Sequence I indicate that these granites are coeval with subalkaline granites of the Taraka pluton (1840 Ma) and the sedimentary protolith of this sequence was formed before the emplacement of the Taraka granitoids. These data, combined with the ages of detrital zircons, presumably modified by metamorphic conditions, suggest that sedimentary rocks of Sequence I were deposited between 1.84 and 1.85 Ga. Unlike the rocks of the Kan complex, the rocks of Sequence I have not experienced granulite-facies metamorphism, the peak of which at 1.87–1.85 Ga, based on the U–Pb age for metamorphic zircon (Urmantseva et al., 2012; Turkina and Sukhorukov, 2015). At the same time, the rocks of Sequence I occurring in the fault, they have been almost synchronously subject to dynamic metamorphism under amphibolite-facies conditions in ductile shear zones (Likhanov et al., 2015b). Sediment accumulation in Sequence I most likely took place before the major Paleoproterozoic orogenic events in the Angara–Kan block.

Table 7. Sm–Nd isotope data on gneisses, schists, metavolcanics, and granite veins, Yenisei complex

No.	Sample No.	Concentration, μg/g		Isotope ratios		*t*, Ma	T_{Nd} (DM), Ma	εNd(*t*)
		Sm	Nd	$^{147}Sm/^{144}Nd$	$^{143}Nd/^{144}Nd$			
1	242-78	33.96	6.82	0.121400	0.511612 ± 2	1850	2530	–1.9
2	283-78	38.60	6.95	0.109000	0.511416 ± 5	1850	2514	–2.7
3	30-09	72.9	12.65	0.104856	0.511359 ± 3	1740	2498	–4.5
4	187-82	47.5	8.35	0.106000	0.511411 ± 22	1740	2452	–3.7
5	158-79	43.01	7.49	0.105285	0.511455 ± 6	1740	2375	–2.7
6	193-82	2.26	10.03	0.135902	0.511709 ± 14	1740	–	–4.6
7	203-79	48.88	8.99	0.111150	0.511658 ± 8	1740	2211	0
8	263-79	29.41	5.09	0.100754	0.511316 ± 13	1850	2555	–3.9
9	288-78	51.9	9.27	0.107815	0.511275 ± 23	1845	2687	–5.6

Note. Sequence I: 1, biotite gneiss; 2, garnet-sillimanite-biotite gneiss. Sequence II: 3, meta-andesite; 4, metadacite; 5, biotite-quartz-feldspar schist; 6, metaleucobasalt. Sequence III: 7, two-mica schist; 8, biotite gneiss; 9, subalkaline granite vein. *T*, age accepted for calculating ε_{Nd}.

The dominance of detrital zircons with an age of 1.86 Ga in the metaterrigenous rocks of paragneiss Sequence IV suggests that the formation of their protoliths succeeded a phase of Paleoproterozoic orogenic activity in the Angara–Kan block, which occurred at 1.87–1.85 Ga, based on the age of metamorphism. The age of the most abundant zircons (1.86 Ga) corresponds to the age (1.87–1.84 Ga) of emplacement of postcollisional granitoids in the southwest of the Siberian craton (Turkina et al., 2006 and others). Two explanations might account for the absence of detrital zircons younger than 1.84 Ga from this sequence, which is considered to be characteristic time interval marking the early stages of emplacement of the Taraka subalkaline granites (Nozhkin et al., 2003). Sediment accumulation might have occurred prior to the emplacement of these granites, or, more likely, the Taraka granites have not yet been uplifted above the erosional surface. Both explanations suggest that the sedimentary rocks of Sequence IV could not be older than 1.86 Ga. Therefore, despite the lithological and geochemical similarity and similar Nd model ages, Sequences I and IV could be diachronous and separated by a stage of Paleoproterozoic orogeny, metamorphism and granite emplacement.

As shown earlier (Nozhkin et al., 2016), the U–Pb age of 1.74 Ga documented by zoned zircons or zircon rims from metaandesites and metadacites of amphibolite-orthogneiss sequence (volcanic) suggests a very large time gap between volcanism and deposition. The difference in the age of metasedimentary and metavolcanic rocks indicates at least a two-stage formation of rock suites, which constitute together the Yenisei metamorphic complex.

Source areas. The trace element composition of metasedimentary rocks of the Yenisei complex indicates a predominantly felsic provenance. The Sm–Nd isotope data for metaterrigenous rocks also indicate a dominant provenance with Neoarchean sialic crust, which is supposed to be similar in composition to the Kan granulite-gneiss complex. This is supported by their similar geochemical characteristics. The enrichment of Th, REE, Zr, and Hf observed in the granulites of the Angara–Kan block and paragneisses of the Yenisei complex (Nozhkin and Turkina, 1993) may indicate that the geochemical signatures of the metasedimentary rocks of the Yenisei complex were inherited from of the eroded granulites. The presence of juvenile Paleoproterozoic crustal material can be inferred only for Sequence III of the Yenisei complex, as indicated by its younger model age and higher ε_{Nd} values (Table 7).

Correlation of metamorphosed sequences. Based on their compositions and stages of their formation, the metasedimentary and metavolcanic rocks of the Yenisei metamorphic complex were previously correlated with metamorphosed volcanosedimentary rocks of the Subluk Group in the Urik–Iya and Elash grabens (Sayan area) and were interpreted to have been formed in the Paleoproterozoic (Nozhkin, 1999). The Urik–Iya and Elash grabens are fragments of an extensive (about 500 km) Paleoproterozoic trough (Bryntsev, 1994) filled with volcanosedimentary successions, which are overlain over much of the area by Riphean deposits of the Karagass and Oselok Groups. New zircon isotope-geochronological data for zircons from granitic veins (~1.85 Ga), detrital zircons from gneisses in sequences I and IV, and earlier data for metavolcanics (1.74 Ga) in Sequence II (Nozhkin et al., 2016) of the Yenisei metamorphic complex provide a more justified approach to their correlation with the sediments of the Urik–Iya and Elash grabens.

The lower, mostly sedimentary part of the section (Ingashi Formation of the Subluk Group) of the Urik–Iya graben is interpreted to have been deposited between 1.91 and 1.87 Ga (Gladkochub et al., 2014) before the emplacement of granitoids (1.87–1.83 Ga). This conclusion is based on their youngest detrital zircon age (1.91 Ga). The discussion of a spatial and temporal relationship between accretionary-collisional events along the southwestern margin of the Siberian Craton is beyond the scope of this study. At the same

time, the emplacement age of granites into Sequence I of the Yenisei complex places the upper limit on a depositional age of this sequence at ~1.85 Ga, which allows us to interpret them to be coeval with the lower part of the Urik–Iya graben section and belonging to the same depositional stage. It is assumed (Gladkochub et al., 2014) that a rift sedimentary basin was formed on the mature continental crust of the Siberian Craton. In the Angara–Kan block, the extensional setting at this stage is documented by the presence of boudinaged sublayers of amphibolites and garnet amphibolites in Sequence I, which are generally conformable to the foliation and have a thickness of 0.5 to 7 m. They were deformed, together with the host paragneisses and calciphyres, by folding and metamorphism. Based on their composition, these rocks are low-aluminous (13.1–14.5 wt.% Al_2O_3) tholeiitic basalts and normal dolerites enriched in CaO (11–13 wt.%). They display flat or LREE-depleted patterns ($(La/Yb)_n$ = 1.0–0.5) and slight LILE enrichment (Rb, Ba, and Th). Their major and trace element geochemistry indicate a depleted mantle source.

The protoliths of Sequence IV of the Yenisei complex were formed during a later period (no older than 1.86 Ga). They have no time equivalents in the rocks of the Urik–Iya graben because the overlying volcanosedimentary strata (Daldarma Formation) are not older than 1.75 Ga. A wide range of terrigenous sediments (from carbonaceous shales to gritstones and conglomerates), extrusive rocks, and tuffs of various compositions were deposited in the second stage (~1.75–1.7 Ga) during an episode of intracontinental extension (Gladkochub et al., 2014). The age of the main peak obtained on detrital zircons from the Daldarma Formation (1845 Ma) suggests that the granitoids of the Sayan complex were the main source of clastic material. The youngest zircons with ages of ~1750 Ma reflect the input of intrusive products of magmatic activity associated with extensional tectonics, which manifested itself in different regions of the southern segment of the Siberian Craton during the late Paleoproterozoic (Bibikova et al., 2001; Turkina et al., 2003; Nozhkin et al., 2009; Gladkochub et al., 2014). In the Angara–Kan block, this stage was marked by the deposition of the amphibolite-orthogneiss (volcanic) sequence containing 1.74 Ga volcanic rocks (Nozhkin et al., 2016). The essentially bimodal character of the volcanic suites of tholeiitic and subalkaline geochemical affinity indicates that they were emplaced in an extensional setting. Based on their emplacement age, these volcanic rocks are correlated with intra-plate granites of the Taraka pluton (Nozhkin et al., 2009). Thus, the metavolcanic suites of Sequence II can be reliably correlated with the volcanosedimentary rocks in the middle part (Daldarma Formation) of the Subluk Group section (Nozhkin et al., 2016). New isotope-geochronological data indicate that the felsic volcanic suites of the Elash graben are noticeably older (1874 ± 10 Ma) (Donskaya et al., 2016) than the volcanics of the Urik–Iya graben and Yenisei complex. They obviously build up the lower, mostly terrigenous part of the section containing metabasalt horizons (Nozhkin, 1999) and were formed during the early stage of formation of the late Paleoproterozoic volcanosedimentary rock associations of the Sayan area.

In general, the metasedimentary and metavolcanic suites of the Yenisei complex, Elash and Subluk Groups can be regarded as a single extensive late Paleoproterozoic Yenisei–Biryusa belt, which can be traced within the Angara–Kan block of the Yenisei Ridge, Elash and Urik–Iya grabens in the Sayan area.

CONCLUSIONS

The results of this study reveal the chemical heterogeneity of the Yenisei metamorphic complex, which represents a series of blocks within the Yenisei Fault of the southern Yenisei Ridge. The Yenisei complex is composed of four metamorphic sequences: amphibolite-marble-paragneiss (volcanic-carbonate-terrigenous), amphibolite-orthogneiss (volcanic), marble-paragneiss (carbonate-terrigenous), and paragneiss (terrigenous).

The study of the nature of the protoliths of metamorphic rocks shows that gneisses and schists of Sequences I and IV correspond to polymictic or arkose sandstones and siltstone-mudstones and can be classified as the first-cycle sediments. Garnet–two-mica schists of Sequence III correspond in their composition to mudstones and show evidence of recycling. The REE and Th content of metasedimentary rocks is 1.2–1.4 times higher than the average PAAS. The high-aluminous varieties have high concentrations of K, Rb, HFSE, Fe, Cr, Ni, and Co. A comparison of the metasedimentary rocks of the Yenisei complex with the spatially associated granulite-facies lithologies of the Kan complex shows that these rocks display a 10–20% difference in the concentrations of most of the trace elements, except for high-aluminous mudstones, which have much higher trace element concentrations. The overall similarity of the average trace element concentrations in the rocks of these two complexes suggests that the composition of the Kan granulites was inherited by metasedimentary rocks of the Yenisei complex.

The U–Pb zircon data for granitic veins cutting the gneisses of amphibolite-marble-paragneiss Sequence I provide constraints on the depositional age of 1.84–1.85 Ga and indicate that these rocks were deposited before the emplacement of postcollision granites of the Taraka pluton. The depositional age of Sequence I (older than 1.85 Ga) predating the main orogenic events in the Angara–Kan block allows us to correlate this sequence with the lower part of the Urik–Iya graben section, which was formed between 1.91 and 1.87 Ga (Gladkochub et al., 2014). The metamorphic rocks from the lower parts of the sections in the Yenisei complex and the Subluk Group were formed during a single rifting phase of sedimentation. The 1.74 Ga amphibolite-orthogneiss (volcanic) sequence was formed during the second stage in the Angara–Kan block of the Yenisei Ridge (Nozhkin et al., 2016). The volcanic rocks were formed in

an extensional setting and can be thus correlated with the emplacement of within-plate granites of the Taraka pluton. In the Sayan area, terrigenous sediments and volcanic rocks of various compositions were deposited in the second stage (1.75–1.7 Ga) during an episode of intracontinental extension. Therefore, there is a good correlation between depositional ages and geodynamic settings of late Paleoproterozoic volcanic and volcanosedimentary complexes of the Yenisei Ridge and Sayan region.

This study was performed as part of the research program of V.S. Sobolev Institute of Geology and Mineralogy, Siberian Branch, Russian Academy of Sciences.

REFERENCES

Bayanova, T.B., 2004. Age of Reference Geologic Complexes in the Kola Region and Duration of Magmatism [in Russian]. Nauka, St. Petersburg.

Bibikova, E.V., Gracheva, T.V., Makarov, V.A., Nozhkin, A.D., 1993. Age constraints in the Early Precambrian geologic evolution of the Yenisei Ridge. Stratigrafiya. Geologicheskaya Korrelyatsiya 1 (1), 35–40.

Bibikova, E.V., Gracheva, T.V., Kozakov, I.K., Plotkina, Yu.V., 2001. U–Pb age of hypersthene granites (kuzeevites) of the Angara–Kan protrusion (Yenisei Range). Geologiya i Geofizika (Russian Geology and Geophysics) 42 (5), 864–867 (823–825).

Bryntsev, V.V., 1994. Precambrian Granitoids of the Northwestern Sayan Area [in Russian]. Nauka, Novosibirsk.

Burg, J.-P., Schmalholz, S.M., 2008. Viscous heating allows thrusting to overcome crustal-scale buckling: Numerical investigation with application to the Himalayan syntaxes. Earth Planet. Sci. Lett. 274 (1–2), 189–203.

Dmitrieva, N.V., Nozhkin, A.D., 2012. Geochemistry of Paleoproterozoic metaterrigenous rocks of the Biryusa Block, southwestern Siberian Craton. Lithol. Miner. Resour. 47 (2), 138–159.

Donskaya, T.V., Gladkochub, D.P., Pisarevsky, S.A., Poller, U., Mazukabzov, A.M., Bayanova, T.B., 2009. Discovery of Archaean crust within the Akitkan orogenic belt of the Siberian craton: New insight into its architecture and history. Precambrian Res. 170 (1–2), 61–72.

Donskaya, T.V., Gladkochub, D.P., Mazukabzov, A.M., Wingate, M.T.D., 2014. Early Proterozoic postcollisional granitoids of the Biryusa block of the Siberian craton. Russian Geology and Geophysics (Geologiya i Geofizika) 55 (7), 812–823 (1028–1043).

Donskaya, T.V., Gladkochub, D.P., Mazukabzov, A.M., Motova, Z.L., Lvov, P.A., 2016. The new Early Proterozoic Sayan–Biryusa volcanoplutonic belt in the southern part of the Siberian Craton, in: Geodynamic Evolution of the Lithosphere of the Central Asian Mobile Belt (from Ocean to Continent), Issue 14 [in Russian]. IZK SO RAN, Irkutsk, pp. 82–84.

Galimova, T.F., Bormotkina, L.A., 1983. Precambrian stratigraphy of the Biryusa block, in: Precambrian Stratigraphy of Central Siberia [in Russian]. Nauka, Leningrad, pp. 125–134.

Galimova, T.F., Permyakov, A.S., Bobrovskii, V.T., Pashkova, L.A., 2011. State Geological Map of the Russian Federation. Scale 1:1,000,000. Sheet N-47, Nizhneudinsk [in Russian]. VSEGEI, St. Petersburg.

Geological Map of the Irkutsk Region and Adjacent Areas, 1985. Scale 1:500,000 [in Russian]. VostSibNIIGGiMS, Irkutskgeologiya. Irkutsk.

Gerya, T.V., Perchuk, L.L., Triboulet, C., Audren, C., Sez'ko, A.I., 1997. Petrology of the Tumanshet zonal metamorphic complex, Eastern Sayan. Petrology 5 (6), 503–533.

Gladkochub, D.P., Mazukabzov, A.M., Stanevich, A.M., Donskaya, T.V., Motova, Z.L., Vanin, V.A., 2014. Precambrian sedimentation in the Urik–Iya Graben, southern Siberian Craton: Main stages and tectonic settings. Geotectonics 48 (5), 359–370.

Kachevskii, L.K. (Ed.), 2002. Legend of the Yenisei Series of the State Geological Map of the Russian Federation, Scale 1: 200000 (second edition) [in Russian]. Krasnoyarskgeologiya, Krasnoyarsk.

Kachevskii, L.K., Kachevskaya, G.I., Storozhenko, A.A., Zuev, V.K., Diner, A.E., Vasil'ev, N.F., 1994. To the question of the allocation of Archean metamorphic complexes in the Transangarian part of the Yenisei Ridge. Otechestvennaya Geologiya 11–12, 45–49.

Kuznetsov, Yu.A., 1988. Petrology of the Precambrian of the Southern Yenisei Ridge. Selected Works, Vol. 1 [in Russian]. Nauka, Novosibirsk.

Levitskii, V.I., Mel'nikov, A.I., Reznitskii, L.Z., Bibikova, E.V., Kirnozova, T.V., Makarov, V.A., Plotkina, Yu.V., 2002. Early Proterozoic postcollisional granitoids in southwestern Siberian craton. Geologiya i Geofizika (Russian Geology and Geophysics) 43 (8), 717–731 (679–692).

Likhanov, I.I., Santosh, M., 2017. Neoproterozoic intraplate magmatism along the western margin of the Siberian Craton: Implications for breakup of the Rodinia supercontinent. Precambrian Res. 300, 315–331.

Likhanov, I.I., Santosh, M., 2019. A-type granites in the western margin of the Siberian Craton: Implications for breakup of the Precambrian supercontinents Columbia/Nuna and Rodinia. Precambrian Res. 328, 128–145.

Likhanov, I.I., Polyansky, O.P., Reverdatto, V.V., Memmi, I., 2004. Evidence from Fe- and Al-rich metapelites for thrust loading in the Transangarian region of the Yenisey Ridge, eastern Siberia. J. Metamorph. Geol. 22 (8), 743–762.

Likhanov, I.I., Kozlov, P.S., Popov, N.V., Reverdatto, V.V., Vershinin, A.E., 2006. Collision metamorphism as a result of thrusting in the Transangara region of the Yenisei Ridge. Dokl. Earth Sci. 411 (1), 1313–1317.

Likhanov, I.I., Nozhkin, A.D., Reverdatto, V.V., Kozlov, P.S., 2014. Grenville tectonic events and evolution of the Yenisei Ridge at the western margin of the Siberian Craton. Geotectonics 48 (5), 371–389.

Likhanov, I.I., Reverdatto, V.V., Kozlov, P.S., Khiller, V.V., Sukhorukov, V.P., 2015a. *P–T–t* constraints on polymetamorphic complexes of the Yenisey Ridge, East Siberia: Implications for Neoproterozoic paleocontinental reconstructions. J. Asian Earth Sci. 113 (1), 391–410.

Likhanov, I.I., Reverdatto, V.V., Kozlov, P.S., Zinoviev, S.V., Khiller, V.V., 2015b. *P–T–t* reconstructions of South Yenisei Ridge metamorphic history (Siberian craton): Petrological consequences and application to the supercontinental cycles. Russian Geology and Geophysics (Geologiya i Geofizika) 56 (6), 805–824 (1031–1056).

Likhanov, I.I., Nozhkin, A.D., Reverdatto, V.V., Kozlov, P.S., Khiller, V.V., 2015c. *P–T* evolution of ultrahigh temperature metamorphism: Evidence for a Late Paleoproterozoic intraplate extension at the southwestern margin of the Siberian Craton. Dokl. Earth Sci. 465 (1), 1139–1142.

Likhanov, I.I., Nozhkin, A.D., Reverdatto, V.V., Krylov, A.A., Kozlov, P.S., Khiller, V.V., 2016. Metamorphic evolution of ultrahigh-temperature Fe- and Al-rich granulites in the south Yenisei Ridge and tectonic implications. Petrology 24 (4), 392–408.

Likhanov, I.I., Nozhkin, A.D., Savko, K.A., 2018a. Accretionary tectonics of rock complexes in the western margin of the Siberian craton. Geotectonics 52 (1), 22–44.

Likhanov, I.I., Régnier, J.-L., Santosh, M., 2018b. Blueschist facies fault tectonites from the western margin of the Siberian Craton: Implications for subduction and exhumation associated with early stages of the Paleo-Asian Ocean. Lithos 304–307, 468–488.

Liu, Y., Gao, S., Hu, Z., Gao, C., Zong, K., Wang, D., 2010. Continental and oceanic crust recycling-induced melt–peridotite interactions in the Trans-North China Orogen: U–Pb dating, Hf isotopes and

trace elements in zircons of mantle xenoliths. J. Petrol. 51 (1–2), 537–571.

Ludwig, K.R., 1999. User's Manual for Isoplot/Ex, Version 2.10: A Geochronological Toolkit for Microsoft Excel. Spec. Publ. Berkeley Geochronology Center, Berkeley.

Ludwig, K.R., 2000. SQUID 1.00: A User's Manual. Spec. Publ. 2, Berkeley Geochronology Center, Berkeley.

Ludwig, K.R., 2003. ISOPLOT 3.00: A Geochronological Toolkit for Microsoft Excel. Spec. Publ. Berkeley Geochronology Center, Berkeley.

Neelov, A.N., 1980. Petrochemical Classification of Metamorphosed Sedimentary and Volcanic Rocks [in Russian]. Nauka, Leningrad.

Nikolaeva, I.V., Palesskii, S.V., Koz'menko, O.A., Anoshin, G.N., 2008. Analysis of geologic reference materials for REE and HFSE by inductively coupled plasma-mass spectrometry (ICP–MS). Geochem. Int. 46 (10), 1016–1022.

Nozhkin, A.D., 1999. Early Proterozoic continent-marginal complexes of the Angara fold belt and their metallogeny. Geologiya i Geofizika (Russian Geology and Geophysics) 40 (11), 1524–1544 (1501–1521).

Nozhkin, A.D., Rikhvanov, L.P., 2014. Radioactive elements in collisional and within-plate sodic-potassic granitoids: accumulation levels and metallogenic significance. Geochem. Int. 52 (9), 740–757.

Nozhkin, A.D., Turkina, O.M., 1993. Geochemistry of Granulites of the Kan and Sharyzhalgai Complexes [in Russian]. OIGGM SO RAN, Novosibirsk.

Nozhkin, A.D., Bibikova, E.V., Turkina, O.M., Ponomarchuk, V.A., 2003. U–Pb, Ar–Ar, and Sm–Nd isotope-geochronological study of porphyritic subalkalic granites of the Taraka pluton (Yenisei Range). Geologiya i Geofizika (Russian Geology and Geophysics) 44 (9), 879–889 (842–852).

Nozhkin, A.D., Turkina, O.M., Maslov, A.V., Dmitrieva, N.V., Kovach, V.P., Ronkin, Yu.L., 2008. Sm–Nd isotopic systematics of Precambrian metapelites from the Yenisei Range and age variations of their provenances. Dokl. Earth Sci. 423 (2), 1495–1500.

Nozhkin, A.D., Turkina, O.M., Bayanova, T.B., 2009. Paleoproterozoic collisional and intraplate granitoids of the southwest margin of the Siberian craton: Petrogeochemical features and U–Pb geochronological and Sm–Nd isotopic data. Dokl. Earth Sci. 428: 1192.

Nozhkin, A.D., Turkina, O.M., Likhanov, I.I., Dmitrieva, N.V., 2016. Late Paleoproterozoic volcanic associations in the southwestern Siberian Craton (Angara–Kan block). Russian Geology and Geophysics (Geologiya i Geofizika) 57 (2), 247–264 (312–332).

Perchuk, L.L., Gerya, T.V., Nozhkin, A.D., 1989. Petrology and retrograde P–T path in granulites of the Kanskaya formation, Yenisey range, Eastern Siberia. J. Metamorph. Geol. 7, 599–617.

Perfil'eva, V.V., Galimova, T.F. (Eds.), 1998. Legend of the East Sayan Series of the State Geological Map of the Russian Federation, Scale 1: 200000 [in Russian]. Irkutskgeologiya, Irkutsk.

Popov, N.V., 2001. Early Precambrian evolution of the South Yenisei Ridge: a tectonic model. Geologiya i Geofizika (Russian Geology and Geophysics) 42 (7), 1028–1041 (972–983).

Postel'nikov, E.S., 1980. Geosynclinal Development of the Yenisei Ridge in the Late Precambrian [in Russian]. Nauka, Moscow.

Rosen, O.M., Condie, K.C., Natapov, L.M., Nozhkin, A.D., 1994. Archaean and Early Proterozoic evolution of the Siberian Craton: a preliminary assessment, in: Condie, K.C. (Ed.), Archaean Crustal Evolution. Elsevier, Amsterdam, pp. 411–459.

Schmalholz, S.V., Podladchikov, Y.Y., 2013. Tectonic overpressure in weak crustal-scale shear zones and implications for the exhumation of high pressure rocks. Geophys. Res. Lett. 40 (10), 1984–1988.

Schuth, S., Gornyy, V.I., Berndt, J., Shevchenko, S.S., Sergeev, S.A., Karpuzov, A.F., Mansfeldt, T., 2012. Early Proterozoic U–Pb zircon ages from basement gneiss at the Solovetsky Archipelago, White Sea, Russia. Int. J. Geosci. 3 (2), 289–296.

Sez'ko, A.I., 1988. The main stages of the evolution of the Sayan continental crust, in: The Precambrian and Paleozoic Evolution of the Earth's Crust [in Russia]. Nauka, Novosibirsk, pp. 7–41.

Sukhorukov, V.P., Gladkochub, D.P., Turkina, O.M., 2018a. The first finding of sapphirine in granulites of the Angara–Kan block: Evidence of ultrahigh-temperature metamorphism in the SW Siberian craton. Dokl. Earth Sci. 479 (2), 443–447.

Sukhorukov, V.P., Turkina, O.M., Tessalina, S., Talavera, C., 2018b. Sapphirine-bearing Fe-rich granulites in the SW Siberian craton (Angara–Kan block): Implication for Paleoproterozoic ultrahigh-temperature metamorphism. Gondwana Res. 57, 26–47.

Taylor, S.R., McLennan, S.M., 1985. The Continental Crust: Its Composition and Evolution. Blackwell, Oxford.

Ten, A.A., 1993. Dynamic model for the generation of high pressures during rock shear (results of a numerical experiment). Dokl. RAN 328 (3), 322–324.

Turkina, O.M., Sukhorukov, V.P., 2015. Stages and conditions of metamorphism of mafic granulites in the Early Precambrian complex of the Angara–Kan terrane (southwestern Siberian Craton). Russian Geology and Geophysics (Geologiya i Geofizika) 56 (11), 1544–1567 (1961–1986).

Turkina, O.M., Bibikova, E.V., Nozhkin, A.D., 2003. Stages and geodynamic settings of Early Proterozoic granite formation on the southwestern margin of the Siberian craton. Dokl. Earth Sci. 389 (2), 159–163.

Turkina, O.M., Nozhkin, A.D., Bayanova, T.B., 2006. Sources and formation conditions of the Early Proterozoic granitoids from the southwestern margin of the Siberian craton. Petrology 14 (3), 262–283.

Urmantseva, L.N., Turkina, O.M., Larionov, A.N., 2012. Metasedimentary rocks of the Angara–Kan granulite-gneiss block (Yenisey Ridge, south-western margin of the Siberian Craton): Provenance characteristic, deposition and age. J. Asian Earth Sci. 49, 7–19.

Vernikovskaya, A.E., Vernikovsky, V.A., Matushkin, N.Yu., Romanova, I.V., Berejnaya, N.G., Larionov, A.N., Travin, A.V., 2010. Middle Paleozoic and Early Mesozoic anorogenic magmatism of the South Yenisei Ridge: first geochemical and geochronological data. Russian Geology and Geophysics (Geologiya i Geofizika) 51 (5), (701–716) 548–562.

Williams, I.S., 1998. U–Th–Pb geochronology by ion-microprobe, in: McKibben, M.A., Shanks III, W.C., Ridley, W.I. (Eds.), Reviews in Economic Geology, Vol. 7: Applications of Microanalytical Techniques to Understanding Mineralizing Processes. Soc. Econ. Geol., Littleton, pp. 1–35.

Xia, X.P., Sun, M., Geng, H.Y., Sun, Y.L., Wang, Y.J., Zhao, G.C., 2011. Quasi-simultaneous determination of U–Pb and Hf isotope compositions of zircon by excimer laser-ablation multiple-collector ICPMS. J. Anal. At. Spectrom. 26, 1868–1871.

Yudovich, Ya.Yu., Ketris, M.P., 2000. Basics of Lithochemistry [in Russian]. Nauka, St. Petersburg.

Editorial responsibility: A.E. Izokh